The Climate of Titan

Jonathan L. Mitchell[1,2] and Juan M. Lora[1]

[1]Department of Earth, Planetary and Space Sciences, University of California, Los Angeles, California 90095; email: jonmitch@ucla.edu, jlora@ucla.edu

[2]Department of Atmospheric and Oceanic Sciences, University of California, Los Angeles, California 90095

Annu. Rev. Earth Planet. Sci. 2016. 44:353–80

The *Annual Review of Earth and Planetary Sciences* is online at earth.annualreviews.org

This article's doi:
10.1146/annurev-earth-060115-012428

Keywords

atmospheres, weather, methane, general circulation, eddies

Abstract

Over the past decade, the Cassini-Huygens mission to the Saturn system has revolutionized our understanding of Titan and its climate. Veiled in a thick organic haze, Titan's visible appearance belies an active, seasonal weather cycle operating in the lower atmosphere. Here we review the climate of Titan, as gleaned from observations and models. Titan's cold surface temperatures (~90 K) allow methane to form clouds and precipitation analogously to Earth's hydrologic cycle. Because of Titan's slow rotation and small size, its atmospheric circulation falls into a regime resembling Earth's tropics, with weak horizontal temperature gradients. A general overview of how Titan's atmosphere responds to seasonal forcing is provided by estimating a number of climate-related timescales. Titan lacks a global ocean, but methane is cold-trapped at the poles in large seas, and models indicate that weak baroclinic storms form at the boundary of Titan's wet and dry regions. Titan's saturated troposphere is a substantial reservoir of methane, supplied by deep convection from the summer poles. A significant seasonal cycle, first revealed by observations of clouds, causes Titan's convergence zone to migrate deep into the summer hemispheres, but its connection to polar convection remains undetermined. Models suggest that downwelling of air at the winter pole communicates upper-level radiative cooling, reducing the stability of the middle troposphere and priming the atmosphere for spring and summer storms when sunlight returns to Titan's lakes. Despite great gains in our understanding of Titan, many challenges remain. The greatest mystery is how Titan is able to retain an abundance of atmospheric methane with only limited surface liquids, while methane is being irreversibly destroyed by photochemistry. A related mystery is how Titan is able to hide all the ethane that is produced in this process. Future studies will need to consider the interactions between Titan's atmosphere, surface, and subsurface in order to make further progress in understanding Titan's complex climate system.

1. INTRODUCTION

Methane: an endogenic source of methane must be present on Titan to resupply the atmosphere, or else the atmosphere and its methane content are "geologically young"

Huygens probe: atmospheric entry probe built by the European Space Agency (ESA) as part of the joint NASA-ESA Cassini-Huygens mission to the Saturn system

DISR: Descent Imager/Spectral Radiometer aboard the Huygens probe

Upon discovering methane in Titan's atmosphere, Gerard Kuiper speculated that Titan's orange color "is due to the action of the atmosphere on the surface itself, analogous to the oxidation supposed to be responsible for the orange color of Mars" (Kuiper 1944, p. 383). We now know that Titan owes its orange hue to the stratospheric haze produced from photolysis of methane (Yung et al. 1984). Such irreversible destruction of methane, mostly into less volatile ethane, was thought to necessitate a global ocean of hydrocarbons (Lunine et al. 1983). That turned out to be wrong as well, as Titan's surface is mostly dry, with liquids sequestered at high latitudes. A question that remains unanswered is, where is all the methane coming from? Perhaps Titan sustains a carbon cycle analogous to Earth's, or some geochemical process gives rise to great, sudden releases of methane (Tobie et al. 2006). Whatever the answer, the long-term stability of Titan's methane reservoir remains uncertain.

This is just one example of many mysteries of Titan's climate system. The senior author of this review (J.L. Mitchell) stumbled into the study of Titan's climate a decade ago, in no small part due to the coincidence between the beginning of his doctoral research and the arrival of the Cassini-Huygens mission at the Saturn system. T0, the first flyby of Titan by Cassini, took place on July 7, 2004. In the few years prior to the Cassini-Huygens arrival, however, ground-based telescopes had already discovered active weather on Titan, and the marvel of adaptive optics allowed determination of its geographical locations. Clouds seemed to be exclusive to the southern hemisphere, which was experiencing summer at the time. How could there be clouds only in the summer hemisphere, given that the long radiative cooling time of Titan's lower atmosphere should average out the seasons (Flasar et al. 1981)? Brown et al. (2002) suggested that surface heating would drive convection that could explain polar cloud observations, and that would change seasonally. Confirmation of this process could be found with a climate model of Titan that included the following essential ingredients: (*a*) atmospheric dynamics, (*b*) radiative transfer, and (*c*) methane thermodynamics (and we describe the mechanism in Section 4.2.2).

In many ways, Titan is the most Earth-like body in the Solar System (other than Earth), but it also has similarities to Mars and Venus. Like Earth, Titan has a thick atmosphere (>1 bar), a moist climate with an active weather cycle (involving methane and perhaps ethane), and stable surface liquids. A strong seasonal cycle dominates Titan's general circulation, as it does on Mars. And Titan's middle atmosphere superrotates (spins faster than the underlying surface) like Venus's. But the cautionary tales above suggest that our collective intuition based on other climates should be critically evaluated. With this in mind, here we aim to summarize the current understanding of Titan's climate, primarily through observations, theory, and climate modeling. We begin with the current observations in Section 2 and proceed to a general discussion of climate theory applied to Titan in Section 3. We then use observations and climate models to diagnose the flow of energy in Titan's climate in Section 4. The role of waves and eddies in Titan's atmosphere is our focus in Section 5. We summarize and offer a list of "big questions" that remain to be addressed in Section 6.

2. CLIMATE OBSERVATIONS

We begin our review with a survey of what is currently known about Titan's climate system from observations, drawing on data gleaned from ground-based and spaceborne observatories, with particular emphasis on the trove of measurements from the Cassini-Huygens mission.

2.1. The Global Energy Budget

During the descent of the Huygens probe through Titan's atmosphere in 2005, the Descent Imager/Spectral Radiometer (DISR) measured methane absorption coefficients (Tomasko et al.

2008a) as well as the vertical distribution and optical properties of Titan's atmospheric haze (Tomasko et al. 2008c). In combination with radiative transfer models, these measurements allowed the accurate calculation of solar radiative heating rates in Titan's low-latitude atmosphere (Tomasko et al. 2008b), which showed that approximately 80% of incident sunlight is absorbed in the atmosphere, and roughly 10% at the surface, in agreement with previous radiative-convective calculations that indicated the existence of greenhouse and antigreenhouse effects on Titan (McKay et al. 1989, 1991). Such single-column models, which suggest Titan's atmosphere is largely in radiative equilibrium (McKay et al. 1989) and have been used to estimate very low surface energy fluxes (McKay et al. 1991, Griffith et al. 2008), are applicable in the global mean, where heating rates balance radiative cooling rates (Tomasko et al. 2008b).

CIRS: Composite Infrared Spectrometer aboard the Cassini spacecraft

In any localized atmospheric column, however, solar and thermal radiative fluxes and the resulting heating and cooling rates are not generally in equilibrium. For instance, at the season and latitude of the Huygens landing, the diurnally averaged solar heating rates exceeded thermal cooling rates everywhere from the surface through the stratosphere, implying that excess heat was being transported out of those latitudes (Tomasko et al. 2008b). Similarly, nonradiative surface fluxes (i.e., turbulent sensible and latent heat exchange) driven by the local surface radiative imbalance were probably considerably larger than those calculated from the global average (Williams et al. 2012).

Indeed, as on Earth, Titan's climate is driven by differential heating: Lower latitudes constantly receive more sunlight than higher latitudes. This inequality produces net heating near the equator, which, in the absence of atmospheric dynamics, would cause the surface temperature gradient between equator and poles to be approximately 20 K (Hourdin et al. 1995). Surface brightness temperatures observed by the Composite Infrared Spectrometer (CIRS) (Jennings et al. 2009) and temperature retrievals from Cassini radio occultations (Schinder et al. 2011, 2012) instead suggest temperature gradients of 2–4 K between the equator and the poles at the surface and lowest layers of the troposphere. Comparisons of tropospheric temperature profiles measured during the Voyager (Lindal et al. 1983) and Cassini-Huygens (Fulchignoni et al. 2005, Schinder et al. 2011) missions also show remarkable constancy, as well as homogeneity at low to mid-latitudes. These observations point to the fact that, in response to differential heating, Titan's atmosphere develops a circulation that acts to transport heat toward the cold polar regions and homogenize temperatures. Unequivocal evidence of this transport also lies in the top-of-atmosphere radiative budget (**Figure 1**). In the absence of transport, Titan's outgoing longwave radiation (OLR) would balance the annual-mean top-of-atmosphere insolation profile, which peaks at the equator and drops by more than 1.5 W m^{-2} toward the poles. In contrast, measurements of Titan's global emitted power show only weak variations with latitude of the OLR, ranging between approximately 2.5 W m^{-2} at the equator and 2.2 W m^{-2} at both poles (Li et al. 2011).

2.2. Observed Climate Zones

Titan appears to be neatly divided into two zones of starkly different climates: low-latitude deserts and high-latitude moist climes (**Figure 2**). At low latitudes, the surface is covered by large swathes of dark dune fields, the vast majority of which occur equatorward of ±30° latitude (Radebaugh et al. 2008). Most of these dunes are longitudinal, observed to flow around topography, and they are thought to be composed primarily of solid organics (Lorenz et al. 2006, Radebaugh et al. 2008). Their presence indicates sufficiently dry conditions to allow wind transport of sediments, as well as a lack of surface liquids that can act as sand traps (Lorenz et al. 2006). In addition to these surface observations, few tropospheric clouds have been observed over Titan's equatorial regions for the duration of the Cassini mission (Rodriguez et al. 2009, Brown et al. 2010, Turtle

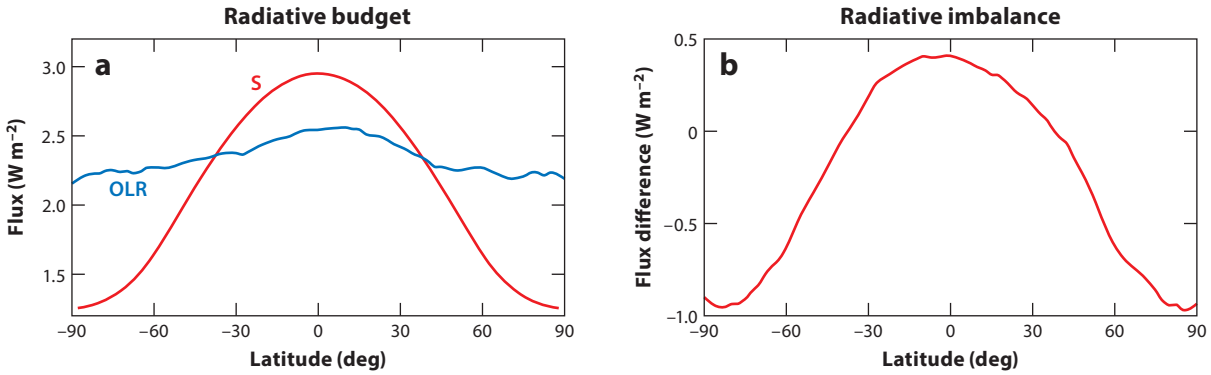

Figure 1

The annual-mean radiative budget at the top of Titan's atmosphere. (*a*) Outgoing longwave radiation (OLR) estimated from Cassini measurements (Li et al. 2011) and annual-mean insolation (S) scaled to be in balance with the OLR. (*b*) The radiative imbalance at the top of the atmosphere, S − OLR.

et al. 2011a). Thus, these low latitudes are generally considered to constitute regions with a desert climate.

In contrast, surface reservoirs of liquid, first revealed by Cassini Radar, abound in Titan's polar regions (Stofan et al. 2007). These include several large seas as well as hundreds of smaller lakes, which mainly occur at northern high latitudes (Hayes et al. 2008). Measurements of the radar loss tangent from Ligeia Mare, the second-largest sea, strongly suggest that the liquid composition is nearly pure methane and ethane (Mastrogiuseppe et al. 2014), implying that these lakes readily interact with the atmosphere and are closely linked to the regional (and probably global) weather and climate. Although Titan's south pole, compared to the north, is relatively devoid of lakes (Aharonson et al. 2009), many lacustrine features, including the large lake Ontario Lacus, have still been identified at high southern latitudes (Turtle et al. 2009). Both polar surfaces are also dotted with features that appear to be empty basins, suggesting geologically recent surface exposures of liquid (Hayes et al. 2008, Aharonson et al. 2009). Importantly, Cassini instruments, as well as ground-based telescopes, detected ample cloud activity over the south pole during its summertime (Brown et al. 2002, 2010; Turtle et al. 2011a), suggesting the presence of high moisture as well as the possibility of rain (Turtle et al. 2009). In combination, these surface and atmospheric features imply that Titan's poles are humid, receive substantial precipitation, and sustain long-lived liquids on their surface, indicating a moist climate.

Other observations of Titan's surface and atmosphere somewhat muddle the simple equator-pole climate dichotomy. First, erosional surface features suggestive of significant liquid flow, including channels and flood plains, have been identified at many different latitudes, including the equatorial regions (Elachi et al. 2005, Tomasko et al. 2005, Lopes et al. 2010). It is possible that at least some of these could be the remnants of a wetter, rainier past climate (Griffith et al. 2008, Moore et al. 2014). Nevertheless, various observations suggest that the present equatorial surface is damp, at least regionally: The Huygens probe detected methane upon landing, presumably from liquid that vaporized as a result of heat from the probe (Niemann et al. 2005); the Visual and Infrared Mapping Spectrometer (VIMS) observed a long-lived black region on the surface nearby the landing site, most consistent with surface liquids (Griffith et al. 2012); and, most recently, nonlinear, supply-limited dune forms were identified and interpreted as arising from interactions with surface liquids (Ewing et al. 2015). Furthermore, observations of enormous cloud outbursts at low latitudes around the vernal equinox (Schaller et al. 2009), and associated surface changes

VIMS: Visual and Infrared Mapping Spectrometer aboard the Cassini spacecraft

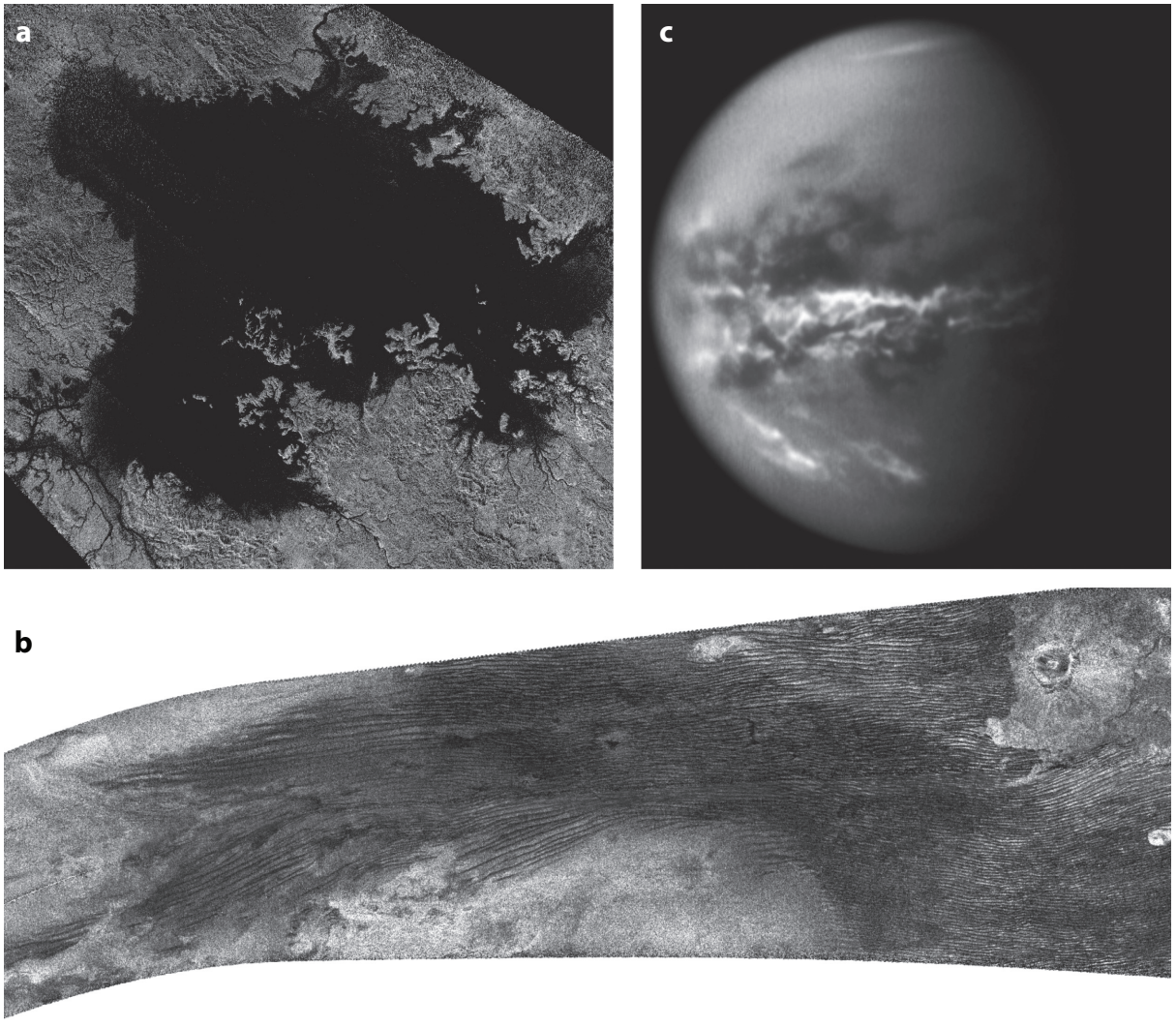

Figure 2

Cassini Radar and Imaging Science Subsystem observations of Titan's surface and lower atmosphere, showing (*a*) Ligeia Mare, one of the large seas at Titan's north pole, (*b*) a large dune field near the equator with dunes flowing around topographic obstacles, and (*c*) tropospheric methane clouds over southern mid-latitudes, the equator, and the north polar regions, shortly after northern vernal equinox. Images courtesy of NASA/JPL-Caltech/ASI/Cornell/Space Science Institute.

probably due to precipitation (Turtle et al. 2011b), as well as common summer cloud activity over southern mid-latitudes (Roe et al. 2005, Griffith et al. 2005), provide even more direct evidence of moisture affecting all latitudes.

2.3. The Methane Cycle

The first solid evidence of Titan's active methane cycle came with the detection of tropospheric clouds in 1995 from ground-based observations, which peered through Titan's obscuring

haze—a phenomenon distinct from cloud formation that is driven by photochemistry in the upper atmosphere—by using near-infrared spectral windows where the atmosphere is relatively transparent (Griffith et al. 1998). Follow-up observations indicated frequent but very sparse (<1% global area) tropospheric cloud cover (Griffith et al. 2000). Adaptive optics then enabled telescopes to resolve Titan well enough to directly image clouds, and these were found clustered over the south pole, which was then in summer, making it apparent that seasonality is an important influence on Titan's weather (Brown et al. 2002, Roe et al. 2002). When Cassini arrived at the Saturn system, both Cassini- and ground-based observations detected a preponderance of tropospheric cloud activity at southern mid-latitudes (Griffith et al. 2005, Porco et al. 2005, Roe et al. 2005), as well as continued cloudiness over the pole (Schaller et al. 2006a). As the season turned from southern summer to northern spring, polar clouds dissipated (Schaller et al. 2006b), mid-latitude clouds persisted (Rodriguez et al. 2009, Brown et al. 2010, Rodriguez et al. 2011, Turtle et al. 2011a), and large storms were observed over the low latitudes (Schaller et al. 2009, Turtle et al. 2011b), confirming a seasonal shift. A much more thorough overview of Titan's observed weather patterns than is possible in this review is offered by Roe (2012) and Griffith et al. (2014), to which the reader is referred.

ISS: Imaging Science Subsystem aboard the Cassini spacecraft

GCMS: Gas Chromatograph Mass Spectrometer aboard the Huygens probe

Though many of the clouds observed on Titan have what appear to be cumulus structures (Porco et al. 2005, Turtle et al. 2011a), only a few cloud heights have been measured. The south polar cloud observed near solstice was estimated to have an altitude of approximately 16 km (Brown et al. 2002), whereas southern mid-latitude clouds were measured to range between approximately 15 and 40 km in altitude (Griffith et al. 2005, Ádámkovics et al. 2010). Simulations with cloud-resolving models have suggested cloud tops generally below 30 km, though surface humidities substantially higher than that observed by Huygens can lead to clouds reaching higher altitudes, up to approximately 40 km, the altitude of the observed temperature minimum (Hueso & Sánchez-Lavega 2006, Barth & Rafkin 2010), suggesting that higher humidities are present at the latitudes observed (Griffith et al. 2014).

Areas of surface darkening, most likely due to precipitation, have been detected by the Imaging Science Subsystem (ISS) in the wake of two large storms, one at the south pole in summertime (Turtle et al. 2009) and a much larger one at low latitudes close to equinox (Turtle et al. 2011b). In the latter case, the observed darkening, which later reverted to its original appearance, was interpreted as surface wetting presumably followed by infiltration and evaporation of the deposited liquid. Based on observations of the northern polar lake regions during late winter, Hayes et al. (2008) suggested surface permeabilities of approximately 10^{-5} to 10^{-6} cm^2 and the possible presence of a relatively shallow methane table to account for a lack of changes. In contrast, summertime observations of the retreat of Ontario Lacus, as well as transience of other small lacustrine features in the south, indicated a significant liquid loss rate of about 1 m yr^{-1} (Hayes et al. 2011). These estimates were further used to approximate precipitation, at least from one summer storm, of approximately 10 cm of methane (Turtle et al. 2011c). All of these values are highly uncertain, but the observations clearly demonstrate the movement of methane between reservoirs that makes up Titan's hydrologic cycle (Lunine & Lorenz 2009).

A fundamental driver of the global methane cycle is the humidity of the troposphere. Prior to Cassini-Huygens, analyses of Voyager data suggested that the troposphere was supersaturated, a situation incompatible with cloud formation if cloud droplets are in equilibrium with the methane vapor (Courtin et al. 1995, Samuelson et al. 1997). The measurement of the methane profile at 10°S by the Huygens Gas Chromatograph Mass Spectrometer (GCMS) demonstrated that no such supersaturation occurred; rather, the relative humidity was found to be 100% from approximately 40 km altitude down to approximately 8 km, with a constant mixing ratio below that indicating a well-mixed, subsaturated lower troposphere (Niemann et al. 2005). The processes that control

the observed surface humidity, ~50%, are uncertain. Griffith et al. (2014) suggested two possibilities: that local buffering of surface methane evaporation by ethane controls this value, or that it is the consequence of a global vapor pressure equilibrium with the northern lakes. Penteado & Griffith (2010) found that low-level methane was roughly constant with latitude between 32°S and 18°N, consistent with the latter hypothesis, whereas Anderson et al. (2008) found evidence of a localized surface source as well as high-latitude, low-level supersaturation. More recently, Ádámkovics et al. (2016) measured the latitudinal profile of methane between 40°S and 80°N via a combination of ground-based and Cassini observations and found an approximately uniform mixing ratio throughout the northern hemisphere and an increase toward the southern hemisphere, suggesting two source regions for moisture, including one in the southern high latitudes (which were in late fall at the time of the observations).

Estimates of the methane reservoir of Titan suggest that unlike on Earth, where water available to the climate system mostly resides in the oceans, the vast majority of methane on Titan resides in the atmosphere (Lorenz et al. 2008). The total atmospheric methane reservoir, if condensed onto the surface, would be roughly 5 m deep (Tokano et al. 2006), whereas Titan's lakes likely contain ~5–10 times less methane (Lorenz et al. 2008, Mastrogiuseppe et al. 2014). The fact that Titan's atmosphere is roughly saturated in methane, which is irreversibly destroyed by photolysis on short timescales (Yung et al. 1984), whereas the observed surface reservoir is vastly insufficient to replenish it, suggests that an unseen subsurface methane source replenishes the atmosphere, or that we are observing Titan at a unique time. A promising candidate for the former option is the presence of a methane (or mixed hydrocarbon) table interacting with subsurface clathrates (Mousis & Schmitt 2008, Choukroun & Sotin 2012). The interaction of such a table with the observable climate system is an outstanding question.

3. THEORETICAL CONSIDERATIONS

Scale analysis of the physical processes that govern climate provides a starting point for understanding the behavior of Titan's climate and atmosphere. **Table 1** lists several important physical constants and parameters for Titan that we use in the following sections.

Table 1 Physical constants for scale analysis of Titan's climate and atmosphere

Parameter symbol	Description	Approximate value
a	Titan's radius	2,575 km
g	Surface gravity	1.35 m s^{-2}
C_p	Specific heat at constant pressure	10^3 J kg^{-1} K^{-1}
$\Gamma_d \equiv g/C_p$	Dry adiabatic lapse rate	1 K km^{-1}
L_v	Latent heat of methane	5×10^5 J kg^{-1}
ρ_l	Liquid methane density	450 kg m^{-3}
Δp_{tropo}	Pressure depth of troposphere	10^3 hPa
T_{tropo}	Tropospheric temperature	80 K
H_{tropo}	Height of troposphere	40 km
Δp_{BL}	Pressure depth of boundary layer	500 hPa
T_{BL}	Boundary layer temperature	90 K
H_{BL}	Height of boundary layer	5 km

Table 2 Climate timescales ordered by increasing value

Description	Equation or reference	Value (years)
Boundary layer radiative	$\tau_{\mathrm{rad,BL}} \simeq \tau_{\mathrm{IR,BL}} \frac{C_\mathrm{p} \Delta p_\mathrm{BL}}{4g\sigma T_\mathrm{BL}^3}$	~7
Shallow overturning	$\tau_{\mathrm{dyn,BL}} \simeq \frac{H_\mathrm{BL}}{T_\mathrm{rad}} \left(\frac{g}{C_\mathrm{p}} - \frac{\Delta T_\mathrm{BL}}{H_\mathrm{BL}} \right)$	~10
Liquid infiltration	Hayes et al. 2008	~10–20
Annual period	$2\pi/\omega_\mathrm{orbit}$	~29.5
Troposphere radiative	$\tau_{\mathrm{rad,tropo}} \simeq \tau_{\mathrm{IR,tropo}} \frac{C_p \Delta p_\mathrm{tropo}}{4g\sigma T_\mathrm{tropo}^3}$	~200
Tropospheric overturning	$\tau_{\mathrm{dyn,tropo}} \simeq H_\mathrm{tropo}/w \simeq \frac{H_\mathrm{tropo}}{T_\mathrm{rad}} \left(\frac{g}{C_\mathrm{p}} - \frac{\Delta T_\mathrm{tropo}}{H_\mathrm{tropo}} \right)$	~500
Methane residence time	$\tau_{\mathrm{CH_4,res}} \simeq \frac{L_\mathrm{v} \times 2{,}250 \text{ kg m}^{-2}}{R}$	~900
Milankovitch cycles	Aharonson et al. 2009	~10^4

3.1. Climate Timescales

A number of timescales related to Titan's climate can be estimated from the available data, as summarized in **Table 2**. The annual period of Titan's seasons is the simplest and most fundamental timescale, set to the orbital period of Saturn around the Sun of 29.5 years, and forms the basis of comparison for all other timescales. First, we consider the radiative relaxation time, which determines how temperatures respond to the seasonal forcing. The infrared optical depth of the troposphere is of order $\tau_{\mathrm{IR,tropo}} \sim 10$ (McKay et al. 1991), so that infrared radiation diffuses through the optically thick troposphere. The time that it takes the troposphere to cool by this process is $\tau_{\mathrm{rad,tropo}} \sim 200$ years, quite a long time compared to the seasonal cycle.

As indicated in **Table 2**, in addition to a dependence on the infrared optical depth $\tau_{\mathrm{IR,tropo}}$, $\tau_{\mathrm{rad,tropo}}$ depends on the pressure depth Δp_tropo and typical temperature T_tropo of the troposphere, which are estimated from the Huygens data (Niemann et al. 2005). The climate system responds to cyclic driving at the orbital frequency (of Saturn) with a thermal inertia related to τ_rad (Mitchell 2008; Pierrehumbert 2010, chapter 7). Normalizing by the orbital frequency of Saturn, $\omega = 2\pi/(29.5 \text{ years}) \sim 7 \times 10^{-9} \text{ s}^{-1}$, we obtain a measure of influence of the seasonal cycle; if $\omega\tau_\mathrm{rad} \gg 1$, seasons are unimportant, whereas if $\omega\tau_\mathrm{rad} \ll 1$, seasons are strong. With $\omega\tau_\mathrm{rad} \sim 1$, seasons are damped in magnitude and lag the forcing by a quarter cycle (Flasar et al. 1981, Mitchell 2008). Because for Titan's troposphere $\omega\tau_\mathrm{rad} \sim 40$, it was previously assumed the troposphere would not experience a seasonal cycle (Flasar et al. 1981, Smith et al. 1981).

However, climate models have now demonstrated a strong seasonal cycle can be present in Titan's troposphere (e.g., Tokano 2005, Mitchell et al. 2006, Lebonnois et al. 2012, Schneider et al. 2012, Lora et al. 2015). How can this be? The answer comes from considering how seasons are communicated to the troposphere: through surface-atmosphere coupling. The surface is subjected to a radiative imbalance as the pattern of insolation shifts with seasons. In the spring, the surface warms faster than the overlying atmosphere, then communicates this warming to the lower atmosphere through boundary layer energy fluxes of sensible and/or latent heat. This creates static instability and drives convection through a depth in the atmosphere dependent on the buoyancy flux at the surface. Models (Tokano et al. 1999, Mitchell et al. 2006, Charnay & Lebonnois 2012, Schneider et al. 2012) and Huygens data (Tokano et al. 2006) suggest the dry boundary layer is only $\Delta p_\mathrm{BL} \sim 500$ hPa (~5 km) thick, and this layer has a smaller optical depth $\tau_{\mathrm{IR,BL}} \sim 1$. Assuming energy transfer is dominated by sensible heat, the dry boundary layer has a radiative

relaxation time of $\tau_{\mathrm{rad,BL}} \sim 7$ years and $\omega\tau_{\mathrm{rad,BL}} \sim 1.5$, so we might expect the dry boundary layer to have a significant seasonal cycle. This is almost certainly the case considering that Titan's weak temperature gradients should allow very small changes in local surface temperatures to drive convection and large-scale overturning (see Section 4.2).

A closely related timescale is the dynamical overturning time of the Hadley circulation. This can be estimated by assuming a thermodynamic balance between compressional heating and radiative cooling in the downwelling branch, where other heat sources and sinks are suppressed,

$$\dot{T}_{\mathrm{rad}} \approx w\left(\Gamma_{\mathrm{d}} - \frac{\partial T}{\partial z}\right) \approx w\left(\frac{g}{C_{\mathrm{p}}} - \frac{\Delta T}{H}\right), \quad (1)$$

where in the last step, the lapse rate is approximated by estimating the temperature drop, ΔT, over a vertical distance H. The overturn time for the entire depth of the troposphere, or the time it takes a parcel to travel a vertical distance H_{tropo}, over which the temperature rises ~15 K (Fulchignoni et al. 2005) while cooling at $\dot{T} \sim 2 \times 10^{-3}$ K Titan day^{-1} (Tomasko et al. 2008b), is $\tau_{\mathrm{dyn,tropo}} \sim 500$ years. Once again, the dry boundary layer has a much shorter overturn time because it is shallow, has a nearly adiabatic lapse rate $\Delta T_{\mathrm{BL}}/H_{\mathrm{BL}} \sim 5.5/6 \sim 0.9$ K km^{-1} (Tokano et al. 2006), and cools slightly faster because of warmer near-surface conditions, $\dot{T}_{\mathrm{rad}} \sim 3 \times 10^{-3}$ K Titan day^{-1} (Tomasko et al. 2008b). Thus, $\tau_{\mathrm{dyn,tropo}} \sim 10$ years. The dry boundary layer evidently responds quite efficiently to seasonal forcing.

To this point, we have ignored the influence of methane in the climate system. However, we know that the atmosphere contains an enormous amount of methane vapor, which if precipitated would amount to a global ocean ~5 m deep. A very large reservoir of latent heat is therefore present in Titan's methane vapor. Methane mixing ratios in the troposphere are in the range $q \sim 10$–20 g kg^{-1} (Niemann et al. 2005), which if entirely condensed could raise the local temperature of the air by $\sim L_{\mathrm{v}} q / C_{\mathrm{p}} \sim 5$–$10$ K. Methane is very clearly an enormous potential source of buoyancy if conditions favor condensation.

As noted above, the imbalance of radiative energy fluxes at the surface drives sensible and/or latent heat fluxes between the surface and atmosphere. One-dimensional (global-average) radiative-convective climate models suggest Titan's atmosphere is very nearly in radiative equilibrium (McKay et al. 1991). Assuming the entirety of the surface radiative imbalance predicted by these models, $R \sim 0.04$ W m^{-2}, goes into evaporating methane, $E \sim R/L_{\mathrm{v}}$, and with a column mass of methane vapor of ~2,250 kg m^{-2}, the residence time of methane is $\tau_{\mathrm{CH_4,res}} \sim 900$ years. One concludes that deep, precipitating convection should be quite a rare phenomenon (Griffith et al. 2008). However, convective methane clouds are relatively common (Rodriguez et al. 2009, Brown et al. 2010, Turtle et al. 2011a). The solution to this apparent paradox is intrinsically two-dimensional, as it involves efficient meridional heat transport in Titan's troposphere (see Section 4). As shown in **Figure 3**, a simulated temperature profile at the location and season of the Huygens descent compares well with the Huygens Atmospheric Structure Instrument (HASI) measurement and appears to be slightly unstable compared with the methane moist adiabat if the lifting condensation level (LCL) is around 3 km altitude (however, the LCL is around 5 km because of the low surface-level relative humidity). The close correspondence between the radiative equilibrium temperature profile and the moist adiabat suggests buoyancy could be easily generated on Titan, for instance by increasing the surface-level relative humidity.

Two additional timescales are of importance to the climate system. On short timescales, methane precipitation may infiltrate into a porous regolith. Using estimates from Huygens probe measurements, Hayes et al. (2008) suggested this should occur over a timescale of $\tau_{\mathrm{infil}} \sim 10$–$20$ years. The correspondence between this timescale and the progression of Titan's seasons

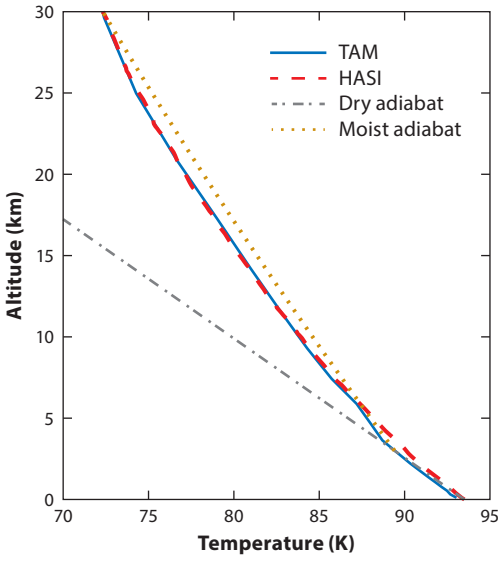

Figure 3

The temperature profile in the Titan Atmospheric Model (TAM) at and during the Huygens descent compared to the Huygens Atmospheric Structure Instrument (HASI) measurement, the dry adiabat, and the methane moist adiabat starting at 3 km altitude.

suggests there may be interesting dynamics at play between seasonal methane weather, soil moisture, and putative subsurface liquid reservoirs.

Finally, Titan experiences long-term variations in insolation and paleoclimate, akin to Earth's well-studied Milankovitch cycles, as a result of changes in Saturn's orbit. The timescale of variations of Saturn's orbital eccentricity, obliquity, and solar longitude of perihelion is $\tau_{\text{orbit}} \sim 4 \times 10^4$ years (Lora et al. 2014). These variations produce changes in the distribution of insolation reaching Titan, and in particular in the contrast of summer insolation between the two poles, which varies with periods of ~45,000 and ~270,000 years and has been proposed to dominate the observed north-south asymmetry of lakes and seas (Aharonson et al. 2009). Over 10^5-year timescales, these insolation differences average out, suggesting that the dominant timescale affecting interhemispheric atmospheric methane transport and the distribution of surface liquids on Titan is $\sim 10^4$ years (Lora et al. 2014). Varying orbital forcing could also produce changes in surface winds at low latitudes, under which dunes would reorient on a timescale of $\sim 10^5$ years (Ewing et al. 2015). Thus, it is possible that various features of Titan's surface record variations of the climate on these longest timescales.

3.2. Force Balances

Scale analysis allows a basic understanding of the fundamental force balances in Titan's atmosphere; these are useful in understanding the class of dynamical flows relevant to the circulation. Perhaps the most basic force balance of relevance to planetary atmospheres is that between gravity and the pressure gradient force, hydrostatic equilibrium, which largely controls the vertical structure of the atmosphere and prevents its collapse or loss to space. In the context of dynamics, hydrostatic balance implies no vertical acceleration of the fluid. For this to be a valid approximation for atmospheric flows, hydrostasy must be nearly satisfied for dynamical perturbations in

density and pressure, as well as for the mean state of the atmosphere (Vallis 2006). This is true when the flow satisfies the condition that

$$\frac{U^2}{L^2 N^2} \ll 1, \tag{2}$$

where U/L is a typical flow advection timescale and N the Brunt-Väisälä frequency. Taking the former to be $\sim 10^{-4}$ to 10^{-5} s^{-1} and the latter to be $\sim 5 \times 10^{-3}$ s^{-1}, it is clear that this condition is thoroughly satisfied for Titan, implying vanishingly small vertical accelerations.

Similar scalings can be applied to the large-scale horizontal flows. On Earth, the dominant force balance is geostrophic, which represents a balance between the Coriolis force and the horizontal pressure gradient. Geostrophic balance occurs when the Rossby number is small. In Titan's stratosphere, which supports strongly superrotating winds (Flasar et al. 1981, Hubbard et al. 1993, Bird et al. 2005, Flasar et al. 2005, Achterberg et al. 2008), the Rossby number is ~10–100, and thus the circulation is predominantly cyclostrophic (Flasar et al. 1981, Flasar & Achterberg 2009), wherein the dominant balance is between pressure gradient and centrifugal forces (Holton 1992). In the troposphere, however, wind speeds are significantly lower, and the balance dynamics are less obvious. Indeed, in the lowest 10 km or so of the troposphere, wind speeds on the order of 1–10 m s^{-1} would imply Rossby numbers roughly one or two orders of magnitude smaller than in the stratosphere, suggesting the possibility of geostrophically balanced flows. The transition between these regimes occurs in the mid-troposphere, where gradient flow involving a three-way balance of the above forces dominates.

Brunt-Väisälä frequency: the frequency of oscillations of an air parcel that is displaced vertically in a statically stable environment

Rossby number: $Ro \equiv U/fL$ is the ratio of inertial to Coriolis forces, a measure of the importance of rotation

4. THE FLOW OF ENERGY IN TITAN'S CLIMATE SYSTEM

It has been recognized for some time that Earth's atmospheric and oceanic general circulation transports heat poleward, such that the tropics are cooler and the extratropics warmer than would be expected from local radiative-convective equilibrium. What is perhaps less obvious is that the energy transport is divided into dry and moist fluxes of (static) energy, and that in the tropics they counteract each other (e.g., Trenberth & Stepaniak 2003). This is a fundamental property of a Hadley circulation, an axisymmetric, thermally direct overturning circulation confined to Earth's tropics (approximately ±30° latitude). The latitudinal extent of Hadley circulations can be understood as the result of poleward angular momentum transport in the upper branch; as axisymmetric rings of air are advected poleward they converge toward the rotation axis, and if we ignore all other torques (primarily friction and eddy stresses, i.e., the inviscid limit), zonal winds must accelerate eastward to conserve angular momentum, thereby producing a subtropical jet. By thermal wind balance, a latitudinal gradient in atmospheric temperatures must be present to balance the Coriolis acceleration on the subtropical jet. The Hadley cell builds the required subtropical temperature gradients by transporting heat out of the deep tropics to the subtropics. Global conservation of energy then provides an upper limit to how large the inviscid Hadley cell can grow (Held & Hou 1980). On Earth, the subtropical temperature gradient is baroclinically unstable, and the instabilities feed back on the mean circulation through concomitant eddy stresses (Schneider 2006). This alters the predicted width of the Hadley cell, but a closed theory including eddy stresses remains to be discovered. In either case, a weaker rotation rate allows the Hadley cell to occupy a larger latitudinal zone because a weaker Coriolis force requires a weaker latitudinal temperature gradient for thermal wind balance. This simple scaling suggests Titan's Hadley cell should be much wider than Earth's, perhaps creating an all-tropics climate dominated by the Hadley circulation (Mitchell et al. 2006).

Because the atmosphere is statically stable, the Hadley circulation transports dry static energy (primarily potential energy) poleward. However, moisture is confined to the lower atmosphere,

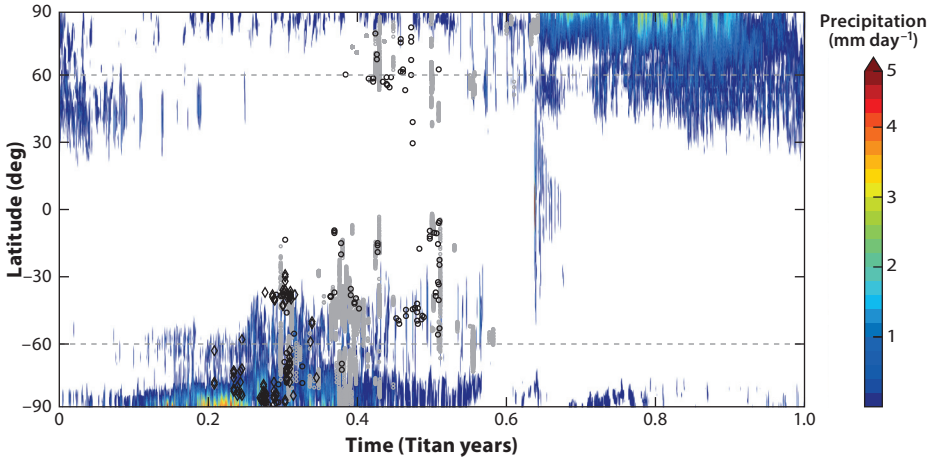

Figure 4

The precipitation distribution (*colors*) from the wetlands simulation with the Titan Atmospheric Model compared to tropospheric cloud locations as observed by the Imaging Science Subsystem (ISS), the Visual and Infrared Mapping Spectrometer (VIMS), and ground-based telescopes. The edges of the wetlands are shown by dashed lines.

where the Hadley circulation converges air toward the equator, and therefore latent energy fluxes of moisture are converged to the equator in the Hadley domain. (In the extratropics, baroclinic eddies transport moisture and dry static energy poleward.) As demonstrated below, Titan's general circulation is dominated by a nearly global Hadley circulation that is highly seasonal, and this has a dramatic effect on the strength of Titan's methane cycle (Mitchell 2012). In what follows, we focus on diagnostics of a particular simulation of Titan's climate with the Titan Atmospheric Model (TAM) (Lora et al. 2015), with specified zones of surface liquid methane poleward of ±60° latitude and dry surface conditions elsewhere (Lora & Mitchell 2015). This wetlands model, as we call it, is motivated by (*a*) the presence of large lakes near Titan's poles and desert-like conditions at low latitudes (see Section 2) and (*b*) the lack of craters poleward of approximately ±60° latitude, implying fast relaxation of surface features by near-surface liquids (Neish & Lorenz 2014). This is the simplest configuration of surface liquids that still produces a precipitation distribution in agreement with that of observed clouds (**Figure 4**).

4.1. Global and Seasonal Considerations

As demonstrated in Section 2.1, the OLR from Titan is considerably flattened in latitude relative to the annual-mean insolation (**Figure 1**). In the annual mean, the top-of-atmosphere radiative imbalance is $R_T \sim 0.5$ W m^{-2} at the equator, which is an order of magnitude larger than the surface radiative imbalance in one-dimensional radiative-convective models of Titan (McKay et al. 1991). Titan general circulation model (GCM) simulations indicate that the majority of R_T is translated into a surface radiative imbalance, R_S, which is available to drive evaporation where liquids are present (Mitchell 2012). The relatively large values of R_T are, in fact, a primary feature missing from radiative-convective climate models that led to a large underestimate of the strength of Titan's methane cycle. Titan's atmosphere efficiently transports heat meridionally on a global scale, essentially erasing the temperature gradient of the troposphere. The large thermal inertia of the atmosphere also holds tropospheric temperatures nearly fixed in time. As a result, the

back-radiation from the atmosphere is lower/higher than it would be in local radiative equilibrium with the annual-mean insolation at low/high latitudes, and the greatest instantaneous surface radiative imbalance occurs at the summer poles (Mitchell 2012). The combined effects of nearly uniform back-radiation from the atmosphere and a significant seasonal cycle of insolation account for local enhancements in R_T of one to two orders of magnitude over the global-mean, radiative-convective prediction.

4.1.1. The implied heat transport. The top-of-atmosphere radiative imbalance, $R_T = \mathrm{S}-\mathrm{OLR}$, in **Figure 1** clearly implies significant meridional heat transport in the atmosphere. Following Trenberth & Stepaniak (2003) and Mitchell (2012) and assuming the surface to be in energy balance, the zonal-mean, column-integrated $[(1/g)\int_0^{p_s}[\cdot]\mathrm{d}p$, here denoted by overbars] thermodynamic equation can be written as

$$\frac{1}{a\cos\varphi}\frac{\partial}{\partial\varphi}(\cos\varphi\overline{F_{M_E}}) = \overline{R}_T, \tag{3}$$

where

$$\overline{F_{M_E}} = \overline{vc_pT} + \overline{v\Phi} + \overline{vLq} \tag{4}$$

is the meridional flux of moist static energy, $\mathrm{MSE} = c_pT + \Phi + Lq$, v is the meridional velocity, Φ is the geopotential, and q is the specific humidity of methane in kg kg^{-1}. Integrating R_T from the south pole, the energy transport of the atmosphere is

$$T_{M_E}(\varphi) = 2\pi a\cos\varphi\overline{F_{M_E}} \tag{5}$$

$$= 2\pi a^2\int_{-\pi/2}^{\varphi} R_T\cos\varphi'\mathrm{d}\varphi'. \tag{6}$$

Figure 5*a* shows T_{M_E} from the integration of R_T in **Figure 1**. We see that Titan's atmosphere transports ~7.5 TW of energy poleward in each hemisphere. From Equation 4, the transport can be accomplished by fluxes of latent energy, Lq, or dry static energy, $c_pT + \Phi$.

Figure 5*b* shows annual-mean T_{M_E} and the components due to latent heat, T_{L_E}, and dry static energy, T_{D_E}, from TAM simulations with surface liquid methane restricted to latitudes poleward of ±60°. Much like in Earth's tropics (Trenberth & Stepaniak 2003), the majority of

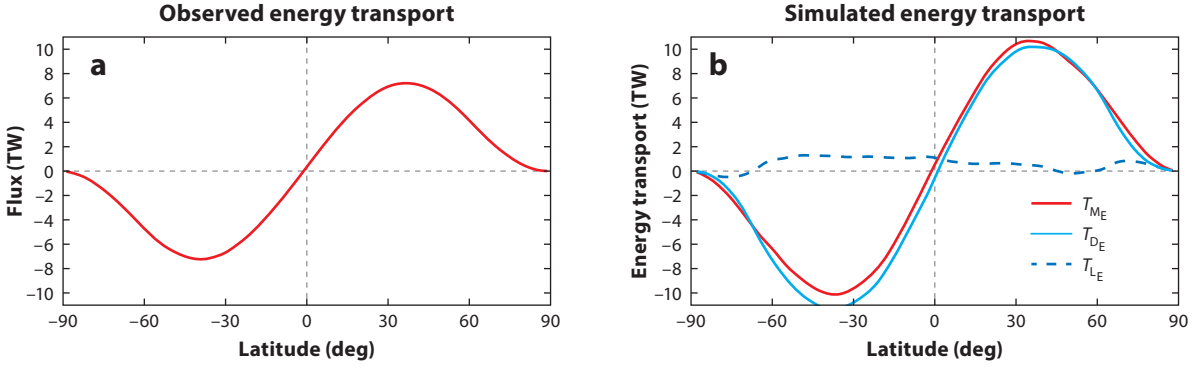

Figure 5

The estimated atmospheric heat flux from integrating Titan's top-of-atmosphere radiative imbalance, R_T, (*a*) estimated from observations and (*b*) derived from the wetlands simulation with the Titan Atmospheric Model.

poleward heat transport is accomplished by dry static energy fluxes, as was also noted by Lora et al. (2015). Inspection of the time variation in global-mean MSE confirms that the equilibrium condition stated in Equation 4 holds for seasonal and longer timescales (not shown). The annual-mean energy transport masks much larger transports that cross the equator and reverse with seasons (Mitchell 2012, Lora et al. 2015). We emphasize here that methane is transported to the summer (warmer) pole by the circulation, and cold trapping of methane refers to the relative reduction in evaporation during wintertime. Furthermore, polar deposition of liquid methane is not hemispherically symmetric, as latent energy fluxes are cross-equatorial at low and intermediate latitudes, and thereby transport a small amount of moisture from the southern to the northern hemisphere (see Section 5 for more on the implications of this hemispheric asymmetry). Poleward of the wetlands, latent fluxes contribute ∼2 TW to the poleward heat transport at high latitudes.

4.1.2. Seasonal amplification of the surface radiative imbalance and methane cycle. Consideration of the arguments in Section 3.1 suggests that Titan's OLR should have only moderate seasonality compared to the insolation, and this appears to be the case (Li 2015). If we also consider the back-radiation from the atmosphere to the surface—the greenhouse effect—to be independent of time and flat in latitude, as is almost certainly the case, then we conclude that a considerable seasonal cycle of radiative imbalance must be present at Titan's surface (Mitchell 2012, Williams et al. 2012). However, this effect is partly offset by the attenuation of shortwave radiation through the slant path of Titan's thick atmosphere at the summer pole (Lora et al. 2011), and the net result is a radiative imbalance of ∼1 W m^{-2} at any given season, as shown in **Figure 6*a***. In the high-latitude region where liquids are present, the TAM simulation responds to radiative heating by evaporating methane, as shown in **Figure 6*b***. The evaporative cooling of methane is significant, such that it tends to reduce surface temperature below the atmospheric boundary layer temperatures, and this results in a reversal of sensible heat fluxes, as shown in **Figure 6*c***. An inverted, stable boundary layer is notoriously difficult to parameterize, because in this situation turbulence is inhibited by the strong static stability (Mitchell et al. 2009), but the effectiveness of the rectification is uncertain. In the present TAM simulation, reversed sensible heat fluxes at summer high latitudes roughly double the amount of evaporation relative to the radiative imbalance. However, better modeling of stable boundary layer energy fluxes will become even more important as detailed studies of Titan's high-latitude meteorology are undertaken, which presents a significant challenge for these studies.

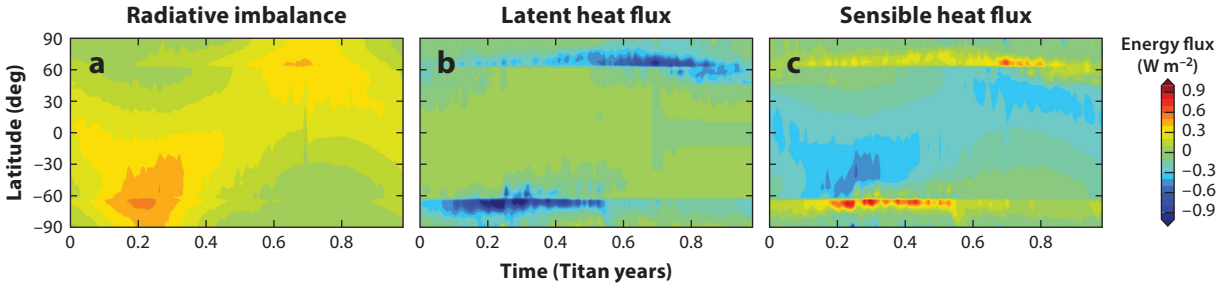

Figure 6

Zonal-mean surface energy fluxes in one year of the wetlands simulation with the Titan Atmospheric Model. Positive fluxes are downward, into the surface. (*a*) Radiative flux imbalance, R_S. (*b*) Surface latent energy flux (i.e., evaporative cooling), E. (*c*) Sensible heat flux.

4.2. Weak Temperature Gradients and Titan's All-Tropics Climate

Measurements of surface brightness temperatures from CIRS suggest the surface is quite uniform in temperature, with variations of ∼1 K between −60° and +60° latitude (Jennings et al. 2009, 2011). Such weak temperature gradients are hallmarks of Earth's tropics and are the result of a weak Coriolis force leading to flattened density, and thus temperature, gradients (e.g., Charney 1963). In the limit of vanishing horizontal temperature gradients, horizontal advection of heat can be neglected, and the steady-state thermodynamic equation leads to a balance between vertical advection of heat and diabatic heating from radiation and convection (Pierrehumbert 1995, Sobel & Bretherton 2000, Williams et al. 2009). On Titan, we expect radiative heating in the troposphere to be essentially time independent except for in the boundary layer, as is also often the case in Earth's tropics.

These considerations suggest that perhaps the simplest climate model for Titan would be a single-column model under the assumption of weak horizontal temperature gradients, and subject to specified variations in insolation and surface energy fluxes. This is essentially the model explored by Williams et al. (2012), who recognized that the back-radiation of Titan's atmosphere to the surface is nearly independent of space and time. The disadvantage of this approach is that horizontal energy transport is treated implicitly by keeping free atmospheric temperatures (above the boundary layer) fixed in time. This is not a major concern in convecting regions of the Earth's tropical oceans, because the magnitudes of horizontally divergent heat fluxes are only a minor contribution to the surface radiative imbalance. However, as shown from the model diagnostics in Section 4.1 (see also Mitchell 2012), it is the horizontal fluxes of energy that are primarily responsible for driving Titan's methane cycle by their effect on the local radiative energy balance of the surface. We suggest a worthwhile endeavor would be to develop an intermediate-complexity climate model involving many atmospheric columns coupled (perhaps diagnostically) through horizontal fluxes of heat and moisture, as this may be necessary to more accurately capture the dynamics of GCMs.

4.2.1. Poleward migration of methane. The absence of a global ocean on Titan is conspicuous and in some ways unexpected, though it was recognized even before Cassini-Huygens (Muhleman et al. 1990). That the atmosphere appears to be a much larger reservoir of methane than the surface (Lorenz et al. 2008) is also curious. But given these two observations, the occurrence of surface liquids at the poles seems to be a natural consequence of the climate system. Titan's atmospheric circulation acts to redistribute methane, drying the low latitudes and delivering moisture to the poles; this behavior is captured in models both with and without an infinite supply of surface methane (Rannou et al. 2006, Mitchell 2008, Schneider et al. 2012, Lora et al. 2015). As discussed in Section 4.1 and shown in **Figure 1**, the annual-mean insolation peaks at the equator and diminishes toward the poles. Surface energy fluxes scale with insolation, and with sufficient surface methane, these are dominated by evaporation (Mitchell 2012, Schneider et al. 2012, Lora et al. 2015). As a result, the potential evaporative loss of surface methane is strongly peaked at low latitudes, and is minimum at the poles. Barring other effects, this polar cold trap causes methane to be more easily retained on the high-latitude surface.

At the same time, seasonal variations cause the top-of-atmosphere insolation to be maximum over the summer poles, such that the radiative imbalance is maximum there for a short time. Though the surface radiative imbalance is not directly proportional to that at the top of the atmosphere (Lora et al. 2011, 2015), it nevertheless exerts a destabilizing influence in the boundary layer at high latitudes during summertime, producing precipitating convection that outpaces any loss due to evaporation (Schneider et al. 2012, Lora et al. 2015). Thus, Titan's polar regions

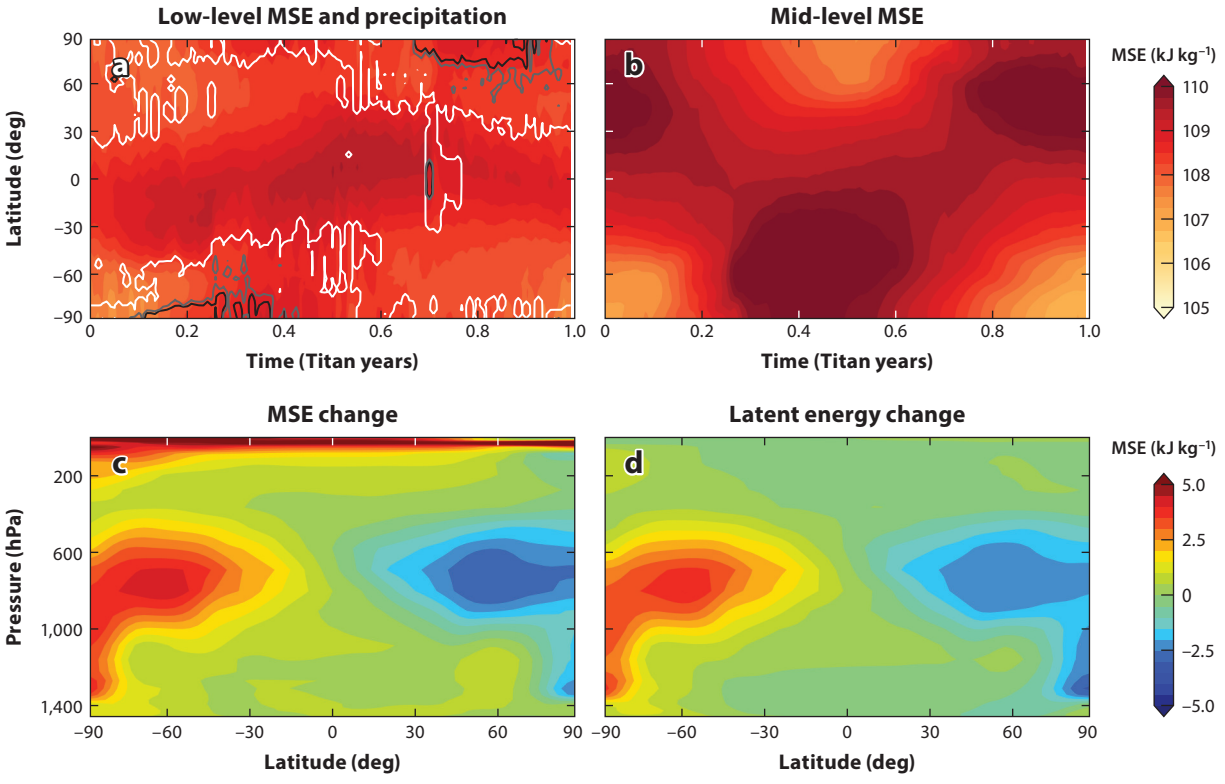

Figure 7

Titan's tropospheric energetics and precipitation in the wetlands simulation using the Titan Atmospheric Model. (*a*) Zonal- and vertical-mean moist static energy (MSE) in the lowest ∼2 km of the model (*color scale*) and precipitation (*black*, 1 mm day^{-1}; *dark gray*, 0.2 mm day^{-1}; *white*, 0.01 mm day^{-1}). (*b*) Zonal- and vertical-mean MSE between 600 and 1,000 mbar (on the same color scale as panel *a*). (*c*) Zonal-mean change in MSE between northern autumnal equinox and northern vernal equinox. (*d*) As in panel *c* for the latent energy, Lq.

receive ample methane rain, which is then relatively stable on the surface, while surface liquids at low latitudes readily evaporate.

4.2.2 Moist static energy and polar deep convection. In Earth's tropics, local maxima in near-surface-level MSE represent a good proxy for where precipitation is likely to occur, and it has been suggested the same may be true for Titan's methane precipitation (Schneider et al. 2012). **Figure 7*a*** shows the zonal-mean vertical-mean MSE in the lowest ∼2 km during one year of the TAM wetlands simulation, along with model precipitation. The summer poles clearly receive the most intense precipitation; however, the low-level MSE is at a local minimum when this precipitation begins. This is also true of polar precipitation in TAM simulations with liquids at all latitudes. The local minimum in MSE is due to the attenuation of shortwave radiation as it passes through a slant path of Titan's atmosphere (Lora et al. 2011). If Titan's climate is all tropics, why then does the maximum MSE argument potentially fail for predicting precipitation?

The answer to this riddle is that an implicit assumption of the maximum MSE argument, namely that the mid-tropospheric value of MSE is nearly constant in space and time, may be violated on Titan. If this assumption held, as it does in Earth's tropics, then deep convection would be favored

in regions with the highest surface-level MSE because those regions would be the least stable (or most unstable) to moist convection. In **Figure 7*b***, the mid-tropospheric MSE is not constant, but varies by several percent at mid- and high latitudes. (Less obvious is that the variation is in quadrature with the insolation, which reflects the long radiative response and overturn times in Titan's mid-troposphere; see Section 3.1.) The winter hemisphere experiences a marked decrease in mid-tropospheric MSE, as shown by the difference in zonal-mean MSE between northern autumnal equinox and northern vernal equinox in **Figure 7*c***. The change in winter-polar, mid-tropospheric MSE is almost entirely due to drying of the mid-levels as shown in **Figure 7*d*** by the difference in the latent energy, Lq, for the same times. Notice also that the summer pole experiences a moistening in this season, and this is due to the deep, precipitating convection occurring there. The seasonal cycle of polar precipitation can be summarized as a sequence of (*a*) wintertime, mid-level tropospheric drying from dry, descending air in the Hadley circulation (and possible condensation during polar night), followed by (*b*) warming and moistening of low-level air as the spring pole becomes illuminated and (*c*) moistening of the mid-level troposphere by deep convection over the summer pole.

For a more direct comparison of the low-level MSE between TAM wetlands and the model of Schneider et al. (2012), **Figure 8** shows the results of a TAM wetlands simulation in which only the liquid-vapor phase transition is considered for methane saturation, keeping all other aspects of the model the same. **Figure 8*c*,*d*** shows that the seasonal change in tropospheric energy in

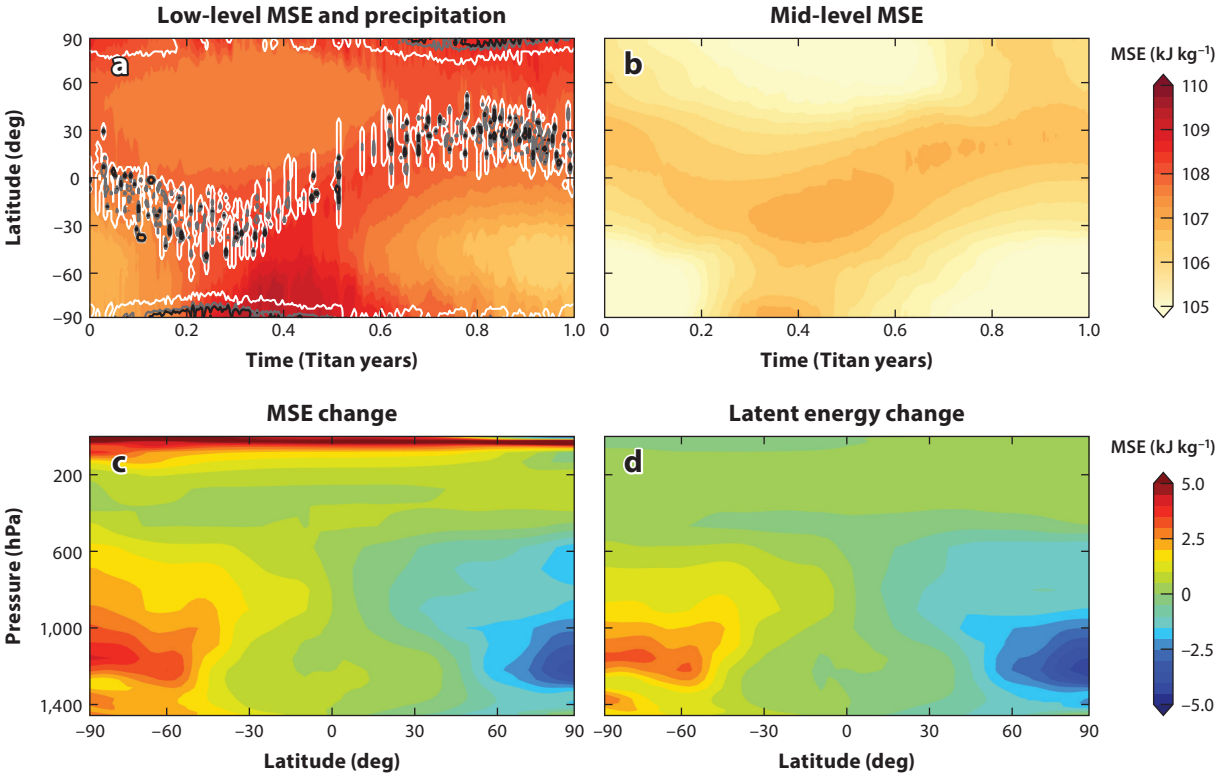

Figure 8

Same as in **Figure 7** for a Titan Atmospheric Model wetlands simulation with methane saturation calculated over liquid only.

this simulation occurs at somewhat lower altitudes than in **Figure 7**. With this parameterization, convective heating is communicated through a shallower layer in less intense and isolated events, so that the circulation is shallower and the outflow from deep, polar convection occurs at a lower level (higher pressure). **Figure 8*a*** also shows that precipitation is weaker and more evenly distributed in season between the seasonally migrating convergence zone and the polar convection. This pattern of precipitation is more consistent with previous model predictions (Mitchell et al. 2006), but not as well matched with the observed clouds (**Figure 4**). It is also now the case that the seasonal pattern of low-level MSE in **Figure 8*a*** has a maximum at the summer poles, as in previous modeling studies (Schneider et al. 2012), although it is not obvious how this comes about. So it seems that the influence of parameterization of methane saturation is an important factor in controlling the intensity and distribution of precipitation, and also the distribution of the low-level atmospheric MSE. But more must be done to understand the exact mechanism(s) responsible for these effects.

4.3. How Titan's Equatorial Region Maintains Low Specific Humidity

It is straightforward to understand how Titan's equatorial region can maintain low relative humidity: The equator is warmer than the poles, surface liquids are present only in the latter region, and so transport of saturated air toward the equator would result in low relative humidity (Griffith et al. 2014). However, recent measurements of the methane concentration—i.e., the specific humidity—suggest that there is actually less methane vapor at low latitudes than at high latitudes (Ádámkovics et al. 2016). This invalidates the hypothesis that Titan's low latitudes are humidified by saturated polar air. As in the observations, the TAM wetlands simulation shows the (low-level) methane concentration increases toward the poles (**Figure 9**). Even accounting for the seasonal cycle in polar temperatures, there is not an obvious way that a saturated air mass originating at the poles could reduce its absolute methane concentration. Instead, we propose the low-latitude, low-level methane concentration is set by the saturated conditions at the top of the dry boundary layer. Titan's equatorial mid-troposphere was observed by Huygens to be saturated from the top of the dry boundary layer to the tropopause (Niemann et al. 2005, Tokano et al. 2006). We suggest the mid-tropospheric specific humidity is kept near saturation by the mid-level outflow from summer polar storms, as **Figure 7*c*** seems to indicate. Collectively, these outflows

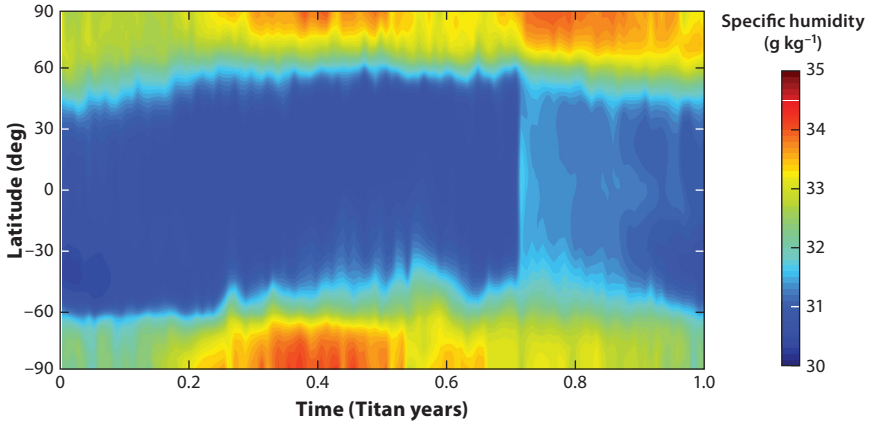

Figure 9

Lowest-model-layer specific humidity for a year of the wetlands Titan Atmospheric Model simulation. A large, equatorial storm at time ∼0.7 (also evident in **Figure 7*a***) transiently humidifies the low latitudes.

represent the upper-level, cross-equatorial branch of Titan's solsticial Hadley circulation. This mid-tropospheric, saturated air mass has a similar effect on warmer regions as having a colder, surface reservoir of evaporating liquids; air parcels that descend from the saturated region compress adiabatically and warm, and thereby conserve their methane specific humidity. In this way, surface-level relative humidity in Titan's low latitudes may be a proxy for the depth of the dry boundary layer.

Virga: wisps or streaks of falling ice or liquid droplets out of a cloud that vaporize before reaching the surface

Cloud-resolving model simulations demonstrate the crucial role played by low-level humidity in generating deep, precipitating convection (Barth & Rafkin 2007, 2010). Large, equatorial storms have been observed (Schaller et al. 2009, Turtle et al. 2011b), but it remains an open question how they are triggered. Some possibilities are (*a*) the humidification by virga from upper levels (Griffith et al. 2009), (*b*) horizontal convergence of vapor transport by the large-scale circulation (Mitchell et al. 2011), and (*c*) localized surface sources of methane. These processes could, in principle, be tested by our TAM wetlands simulation, because a large equatorial storm is produced at time ∼0.7 in the year, presented in **Figure 7*a***. But we leave this as an open question.

5. THE ROLES OF WAVES AND EDDIES

We have already discussed an important aspect of Titan's general circulation, the Hadley circulation. A Hadley cell is axisymmetric, and to this point we have ignored the influence of nonaxisymmetric motions of the atmosphere. This was certainly a good place to start, given that Titan's general circulation is likely to be dominated by a Hadley circulation. But the presence of superrotation in Titan's stratosphere is a smoking gun for the importance of nonaxisymmetric disturbances, which we refer to as waves and eddies.

To achieve and sustain superrotation, where the angular momentum of the atmosphere exceeds that of the solid body at the equator, angular momentum must be transported upgradient in the atmosphere. This can be accomplished by nonaxisymmetric waves (Gierasch 1975, Rossow & Williams 1979) that generally originate in regions of barotropic or mixed barotropic-baroclinic instability (Mitchell & Vallis 2010). Such waves have been studied in the stratospheres of three-dimensional Titan GCMs (Hourdin et al. 1995, Newman et al. 2011), as well as parameterized in axisymmetric circulation models to capture some of their mixing effects on momentum and tracers (i.e., Luz et al. 2003). A more detailed overview of that work, for which the reader is referred to Müller-Wodarg et al. (2014) and references therein, is outside the scope of this review.

Eddies and momentum transport in Titan's troposphere have received considerably less attention than in the stratosphere, presumably because of a lack of observations. Recent analysis of three-dimensional simulations using the Institut Pierre Simon Laplace Titan GCM showed sustained poleward transport of angular momentum by eddies in the lower troposphere (Lebonnois et al. 2012). It was suggested that these eddies are baroclinic based on the dynamical regime of the flow in that part of the atmosphere, although the condition for baroclinic instability was not demonstrated. Similarly, the influence of wave activity on the methane cycle has only recently been investigated, though its impacts are likely significant. We now turn our focus to the little-studied role of waves and eddies in Titan's troposphere.

5.1. Eddy Influence on the Methane Cycle

In Titan's all-tropics climate, we might expect equatorially trapped wave modes (Matsuno 1966) to play a role in organizing convection, as they do in Earth's tropics (Wheeler & Kiladis 1999). Observations of these modes are difficult, because clouds are relatively infrequent in Titan' low latitudes. Three large equatorial storms have been observed, the first from ground-based

observations (Schaller et al. 2009). A significant cloud was first observed at southern low latitudes, which then propagated eastward and southward, finally triggering a large cloud outburst near the south pole. The mode was interpreted as a meridionally propagating Rossby wave excited by convection (Schaller et al. 2009). A second set of very large storms with equatorial components was observed by ISS in 2010 (Turtle et al. 2011a), and one caused changes in surface albedo interpreted as wetting by precipitation (Turtle et al. 2011b). Analysis with a Titan GCM at the concurrent season showed that the morphologies of these latter two storms represent the leading two modes of variability in the model simulations, and the modes correspond to an equatorial Kelvin wave and a mixed mode involving high-latitude Rossby waves interacting with an equatorial mode (Mitchell et al. 2011). These analyses further support the notion that tropical atmospheric dynamics play an important role in Titan's climate and weather.

Though, as discussed above and described by several modeling studies (Rannou et al. 2006; Mitchell 2008; Schneider et al. 2012; Lora et al. 2014, 2015), the separation of climates between Titan's low and high latitudes, and the associated preponderance of surface liquids at the latter, neatly arises as a result of the mean circulation and its transport of energy, the same is not true of the significant asymmetry between the observed liquid reservoirs of the north and south poles. This asymmetry is suggested to be a consequence of variations in Saturn's orbit that lead to Titan's equivalent of Milankovitch cycles (Aharonson et al. 2009). Three-dimensional GCMs have shown that surface methane does preferentially build up in the north in the current epoch (Schneider et al. 2012, Lora et al. 2014), and simulations including orbital parameter variations over the past 42,000 years have further shown that the hemisphere to which methane migrates varies with the north-south contrast in summer insolation, oscillating between north and south (Lora et al. 2014).

Hemispheric, annual-mean asymmetries of both evaporation (Aharonson et al. 2009) and precipitation (Schneider et al. 2012) have been proposed as the process responsible for generating the asymmetry of total liquids, but given Titan's finite methane reservoir, both also imply an asymmetric transport of methane between hemispheres by the atmosphere. That previous axisymmetric models studying the distribution of liquids (i.e., Mitchell 2008) did not find an obvious asymmetry is a telltale implication of three-dimensional eddies in this transport, which such models cannot resolve. Recently, analysis of moisture transport by different components of the (present-day) methane cycle in the TAM wetlands simulations revealed that a significant equatorward moisture flux of methane in the atmosphere, with little seasonal variation, is produced by transient, nonaxisymmetric eddies at mid- to high latitudes, whereas the mean meridional circulation is responsible for highly seasonal high-latitude poleward transport and cross-equatorial low latitude transport of methane (Lora & Mitchell 2015). In the annual mean, the combination of these components produces the total moisture flux shown in **Figure 5**, where the net northward transport equatorward of ~70°S in the southern hemisphere is not mirrored in the north. The eddy transport, which feeds methane from the polar regions into the cross-equatorial Hadley circulation, is stronger over southern high latitudes, producing this asymmetric net transport. In the simulations, the southern polar surface reservoir experienced a net loss of methane, whereas the north gained methane, demonstrating that the nonlinear eddy response to solar heating mediates the methane asymmetry and provides a mechanism for Titan's climate system to respond to variations in orbital forcing. The nature of the eddies responsible for this transport is described in more detail in the following section.

5.2. Tropospheric Instabilities

Thus far we have considered the effect of waves and eddies on the climate and general circulation. But from where do the eddies and waves draw their energy? Many three-dimensional Titan GCMs

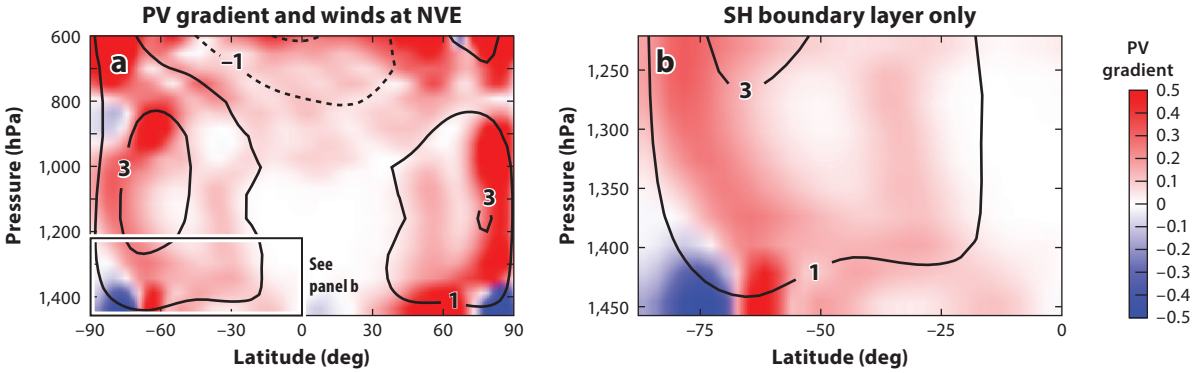

Figure 10

Zonal-mean potential vorticity (PV) gradient (*shading*; arbitrary units) and zonal-mean zonal winds (*black contours*; m s^{-1}) just after northern vernal equinox from (*a*) 600 mbar to the surface and in both hemispheres and (*b*) 1,200 mbar to the surface and southern hemisphere only.

(Hourdin et al. 1995, Mitchell et al. 2011, Lebonnois et al. 2012, Lora & Mitchell 2015) that see nonaxisymmetric activity, including the TAM wetlands simulation we employ here, use entirely axisymmetric boundary conditions and forcing, and therefore any nonaxisymmetric disturbances arise spontaneously from instabilities. One possibility is convective instability, which we discussed previously in Section 4.2.2 as playing an important role in Titan's summer polar precipitation. Another possibility is barotropic instability, which is thought to play a primary role in maintaining Titan's superrotating stratosphere, as discussed above. Here we focus our attention on the lower atmosphere at high latitudes, below 600 mbar and poleward of 45° latitude, where winds peak at ∼5 m s^{-1} to give a global-scale Rossby number of ∼0.1, such that our notions of fluid instabilities in the quasi-geostrophic system should apply (Vallis 2006). A necessary condition for barotropic instability is that the gradient of the potential vorticity reverse from one latitude to another (the so-called Rayleigh-Kuo criterion; Vallis 2006). In **Figure 10*a***, the gradient of the potential vorticity (PV) for the primitive equations from 600 mbar to the surface in the TAM simulation just after northern vernal equinox shows such a reversal at the southern high latitudes, and this may indicate a role for barotropic instability in Titan's tropospheric dynamics. However, the process of cyclogenesis, by which Earth's mid-latitude storms produce frontal lifting (weather), requires baroclinic instability. A necessary condition for baroclinic instability is the presence of a PV gradient reversal from one level to another, i.e., in the vertical direction (Vallis 2006). Typically, the PV gradient reversal occurs at low levels in a region of concentrated surface temperature gradients. **Figure 10*b*** shows the PV gradient from 1,200 mbar to the surface (roughly the depth of the dry boundary layer) in the summer hemisphere just after northern vernal equinox. There is evidence of a PV gradient reversal in the vertical from ∼60°S to the pole, indicating that baroclinic instability may be present here at this season.

Inspection of the nonaxisymmetric component of the specific humidity and winds at these latitudes in **Figure 11*a*** indicates the presence of a zonal-wavenumber-1 disturbance with a westward tilt in the vertical, a hallmark of baroclinic storms. The disturbance is quite shallow, however, and only extends through the dry boundary layer. This can be understood by the following argument based on the influence of the static stability: Cyclogenesis preferentially occurs at the deformation radius, $L_D = NH/f$, with Brunt-Väisälä frequency N, scale height H, and Coriolis parameter f (see **Table 3**). In Earth's mid-latitudes, $L_D \sim 1{,}000$ km. However, if we were to estimate L_D for characteristic values of Titan's high-latitude troposphere, we would find $L_D > a$, i.e., larger than

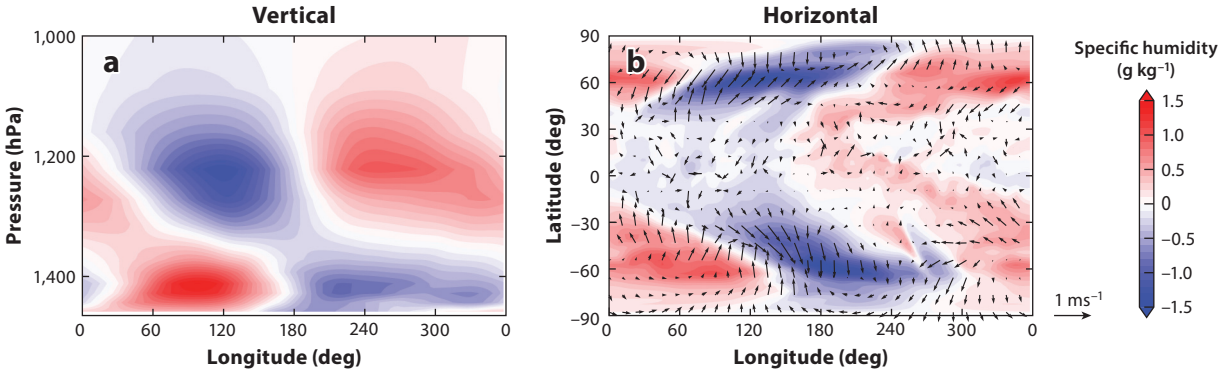

Figure 11

Zonal-wavenumber-1, baroclinic eddies are shown in (*a*) pressure-longitude cross section of specific humidity anomalies and (*b*) latitude-longitude cross section of low-level specific humidity anomalies (*shading*) and surface winds (*arrows*). For a video of these images, see the **Supplemental Material**.

Supplemental Material

Rossby radius of deformation: $L_D \sim NH/f$ estimates the length scale a wave can travel before being affected by rotation

Titan itself. If we instead assume cyclogenesis occurs at the largest horizontal scales, $L_D \sim a$, then we conclude the modes will also have to be quite shallow, confined to the lowest ∼5 km of the troposphere. We can then estimate the time it takes for this mode to grow by the Eady timescale, $T_{Eady} = a/U \sim 10^6$ s, for a mode with horizontal scale $a = 2{,}575$ km and imbedded in a shear zone with zonal-mean zonal wind at H of magnitude $U \sim 3$ m/s. Apparently, baroclinic modes would have sufficient time to significantly grow in amplitude in a single Titan day. **Figure 11*b*** shows that the disturbance also has a northwest-southeast tilt in the horizontal, with some evidence of frontal development (convergent winds between warm and cold air masses). These are all characteristic of baroclinic storms. Thus, we conclude that, like in Earth's mid-latitudes, Titan's mid- and high-latitude weather systems may be the result of baroclinic instability.

6. SUMMARY AND QUESTIONS

Titan's tropospheric circulation at summer solstice is dominated by a deep and relatively sluggish Hadley circulation extending from the summer to the winter pole, while more intense but shallower circulations are split into multiple cells in the dry boundary layer below ∼1,000 hPa. The deep circulation exports relatively warm, moistened air from the summer polar surface into the southern high- and low-latitude upper troposphere. This has two main effects on the low latitudes: (*a*) Because the latitudinal temperature gradient is weak, the middle troposphere essentially fills with saturated air, as observed; and (*b*) the low latitudes are maintained in a relatively statically stable state, consistent with low cloud heights there. In the winter hemisphere, the descending

Table 3 Radius of deformation on Earth and Titan

Parameter	Earth	Titan
Brunt-Väisälä frequency, N (s^{-1})	10^{-2}	5×10^{-3}
Scale height, H (km)	7	20
Coriolis parameter, f (s^{-1})	10^{-4}	10^{-5}
Deformation radius, L_D (km)	700	10^4
Confinement height, H_c (km)	NA	5

branch imports dry air into the mid-troposphere over the winter pole, while the downwelling air that is cooled radiatively reduces the stability over the winter polar atmosphere. This primes the pump for the winter polar region to produce deep convection in the spring and summer when evaporation from surface reservoirs triggers deep convection. These processes then reverse direction during the next solstice, as described in Section 4.2.2.

SUMMARY POINTS

1. Titan's climate is all tropics except for weak baroclinic storms at the high-latitude boundary between dry and wet zones.
2. Methane is cold trapped at the poles. A hemisphere-switching asymmetry in surface liquids results from Milankovitch cycles, but only does so with the aid of three-dimensional eddies.
3. Energy transport by Titan's global overturning circulation, evident from measurements of the outgoing longwave radiation, produces local radiative imbalances that drive an active weather cycle, despite relatively weak radiative forcing from the Sun. Surface evaporative energy fluxes are at least ten times larger than estimates based on one-dimensional, radiative-convective models.
4. Titan's middle troposphere, saturated by outflow from deep polar storms, supplies the low-latitude boundary layer with low methane concentration.
5. A troposphere-filling overturning circulation switches direction with seasons, transports dry air downward over the winter pole, and reduces the atmospheric stability. This primes the winter pole for spring and summer convection when sunlight returns to the high-latitude lakes.

FUTURE ISSUES

Titan climate models have proven successful at reproducing many of the phenomena discussed in Section 2, and analysis of the model simulations have given us deeper insight into the workings of Titan's climate. The most interesting and opportune areas of research, however, are where expectations from theory and models fail to account for some phenomenon. Many such research areas remain to be explored, and we offer a few examples here.

1. How does Titan's global topography interact with its weather and climate?
2. What is the trigger for large equatorial storms?
3. Where is all the ethane, and how does it affect the methane cycle?
4. How wet is the surface? How does a subsurface alkanofer interact with Titan's methane cycle?
5. How should turbulent surface energy fluxes be parameterized in statically stable conditions over the lakes?
6. How important are the phase and composition of cloud particles to deep convection and the overall circulation?

DISCLOSURE STATEMENT

The authors are not aware of any affiliations, memberships, funding, or financial holdings that might be perceived as affecting the objectivity of this review.

ACKNOWLEDGMENTS

We gratefully acknowledge the Cassini-Huygens team for inspiring this work. We acknowledge informative conversations with Rodrigo Caballero, David Neelin, Máté Ádámkovics, Elizabeth Turtle, and Caitlin Griffith. We thank Sébastien Rodriguez for providing the distribution of VIMS cloud observations. This work was partially supported by NASA grants NNX12AI71G and NNX12AM81G, and TAM was developed with support from the Cassini project and NASA fellowship NNX12AN79H.

LITERATURE CITED

Achterberg RK, Conrath BJ, Gierasch PJ, Flasar FM, Nixon CA. 2008. Titan's middle-atmospheric temperatures and dynamics observed by the Cassini Composite Infrared Spectrometer. *Icarus* 194:263–77

Ádámkovics M, Barnes JW, Hartung M, de Pater I. 2010. Observations of a stationary mid-latitude cloud system on Titan. *Icarus* 208:868–77

Ádámkovics M, Mitchell JL, Hayes AG, Rojo PM, Corlies P, et al. 2016. Meridional variation in tropospheric methane on Titan observed with AO spectroscopy at Keck and VLT. *Icarus* 270:376–88

Aharonson O, Hayes AG, Lunine JI, Lorenz RD, Allison MD, Elachi C. 2009. An asymmetric distribution of lakes on Titan as a possible consequence of orbital forcing. *Nat. Geosci.* 2:851–54

Anderson CM, Young EF, Chanover NJ, McKay CP. 2008. HST spectral imaging of Titan's haze and methane profile between 0.6 and 1 μm during the 2000 opposition. *Icarus* 194:721–45

Barth EL, Rafkin SCR. 2007. TRAMS: a new dynamic cloud model for Titan's methane clouds. *Geophys. Res. Lett.* 34:L03203

Barth EL, Rafkin SCR. 2010. Convective cloud heights as a diagnostic for methane environment on Titan. *Icarus* 206:467–84

Bird MK, Allison M, Asmar SW, Atkinson DH, Avruch IM, et al. 2005. The vertical profile of winds on Titan. *Nature* 438:800–2

Brown ME, Bouchez AH, Griffith CA. 2002. Direct detection of variable tropospheric clouds near Titan's south pole. *Nature* 420:795–97

Brown ME, Roberts JE, Schaller EL. 2010. Clouds on Titan during the Cassini prime mission: a complete analysis of the VIMS data. *Icarus* 205:571–80

Charnay B, Lebonnois S. 2012. Two boundary layers in Titan's lower troposphere inferred from a climate model. *Nat. Geosci.* 5:106–9

Charney JG. 1963. A note on large-scale motions in the tropics. *J. Atmos. Sci.* 20:607–9

Choukroun M, Sotin C. 2012. Is Titan's shape caused by its meteorology and carbon cycle? *Geophys. Res. Lett.* 39:L04201

Courtin R, Gautier D, McKay CP. 1995. Titan's thermal emission spectrum: reanalysis of the Voyager infrared measurements. *Icarus* 114:144–62

Elachi C, Wall S, Allison M, Anderson Y, Boehmer R, et al. 2005. Cassini Radar views the surface of Titan. *Science* 308:970–74

Ewing RC, Hayes AG, Lucas A. 2015. Sand dune patterns on Titan controlled by long-term climate cycles. *Nat. Geosci.* 8:15–19

Flasar FM, Achterberg RK. 2009. The structure and dynamics of Titan's middle atmosphere. *Philos. Trans. R. Soc. A* 367:649–64

Flasar FM, Achterberg RK, Conrath BJ, Gierasch PJ, Kunde VG, et al. 2005. Titan's atmospheric temperatures, winds, and composition. *Science* 308:975–78

Flasar FM, Samuelson RE, Conrath BJ. 1981. Titan's atmosphere: temperature and dynamics. *Nature* 292:693–98
Fulchignoni M, Ferri F, Angrilli F, Ball AJ, Bar-Nun A, et al. 2005. In situ measurements of the physical characteristics of Titan's environment. *Nature* 438:785–91
Gierasch PJ. 1975. Meridional circulation and the maintenance of the Venus atmospheric circulation. *J. Atmos. Sci.* 32:1038–44
Griffith CA, Hall JL, Geballe TR. 2000. Detection of daily clouds on Titan. *Science* 290:509–13
Griffith CA, Lora JM, Turner J, Penteado PF, Brown RH, et al. 2012. Possible tropical lakes on Titan from observations of dark terrain. *Nature* 486:237–39
Griffith CA, McKay CP, Ferri F. 2008. Titan's tropical storms in an evolving atmosphere. *Astrophys. J.* 687:L41–44
Griffith CA, Owen T, Miller GA, Geballe T. 1998. Transient clouds in Titan's lower atmosphere. *Nature* 395:575–78
Griffith CA, Penteado P, Baines K, Drossart P, Barnes J, et al. 2005. The evolution of Titan's mid-latitude clouds. *Science* 310:474–77
Griffith CA, Penteado P, Rodriguez S, Le Mouélic S, Baines KH, et al. 2009. Characterization of clouds in Titan's tropical atmosphere. *Astrophys. J.* 702:L105–9
Griffith CA, Rafkin S, Rannou P, McKay CP. 2014. Storms, clouds, and weather. See Müller-Wodarg et al. 2014, pp. 190–223
Hayes A, Aharonson O, Callahan P, Elachi C, Gim Y, et al. 2008. Hydrocarbon lakes on Titan: distribution and interaction with a porous regolith. *Geophys. Res. Lett.* 35:L09204
Hayes AG, Aharonson O, Lunine JI, Kirk RL, Zebker HA, et al. 2011. Transient surface liquid in Titan's polar regions from Cassini. *Icarus* 211:655–71
Held IM, Hou AY. 1980. Nonlinear axially symmetric circulations in a nearly inviscid atmosphere. *J. Atmos. Sci.* 37:515–33
Holton JR. 1992. *An Introduction to Dynamical Meteorology*. San Diego: Academic. 3rd ed.
Hourdin F, Talagrand O, Sadourny R, Courtin R, Gautier D, McKay CP. 1995. Numerical simulations of the general circulation of the atmosphere of Titan. *Icarus* 117:358–74
Hubbard WB, Sicardy B, Miles R, Hollis AJ, Forrest RW, et al. 1993. The occultation of 28 Sgr by Titan. *Astron. Astrophys.* 269:541–63
Hueso R, Sánchez-Lavega A. 2006. Methane storms on Saturn's moon Titan. *Nature* 442:428–31
Jennings DE, Cottini V, Nixon CA, Flasar FM, Kunde VG, et al. 2011. Seasonal changes in Titan's surface temperatures. *Astrophys. J.* 737:L15
Jennings DE, Flasar FM, Kunde VG, Samuelson RE, Pearl JC, et al. 2009. Titan's surface brightness temperatures. *Astrophys. J.* 691:L103–5
Kuiper GP. 1944. Titan: a satellite with an atmosphere. *Astrophys. J.* 100:378–83
Lebonnois S, Burgalat J, Rannou P, Charnay B. 2012. Titan global climate model: a new 3-dimensional version of the IPSL Titan GCM. *Icarus* 218:707–22
Li L. 2015. Dimming Titan revealed by the Cassini observations. *Sci. Rep.* 5:8239
Li L, Nixon CA, Achterberg RK, Smith MA, Gorius NJP, et al. 2011. The global energy balance of Titan. *Geophys. Res. Lett.* 38:L23201
Lindal GF, Wood GE, Hotz HB, Sweetnam DN, Eshleman VR, Tyler GL. 1983. The atmosphere of Titan—an analysis of the Voyager 1 radio occultation measurements. *Icarus* 53:348–63
Lopes R, Stofan E, Peckyno R, Radebaugh J, Mitchell K, et al. 2010. Distribution and interplay of geologic processes on Titan from Cassini Radar data. *Icarus* 205:540–58
Lora JM, Goodman PJ, Russell JL, Lunine JI. 2011. Insolation in Titan's troposphere. *Icarus* 216:116–19
Lora JM, Lunine JI, Russell JL. 2015. GCM simulations of Titan's middle and lower atmosphere and comparison to observations. *Icarus* 250:516–28
Lora JM, Lunine JI, Russell JL, Hayes AG. 2014. Simulations of Titan's paleoclimate. *Icarus* 243:264–73
Lora JM, Mitchell JL. 2015. Titan's asymmetric lake distribution mediated by methane transport due to atmospheric eddies. *Geophys. Res. Lett.* 42:6213–20
Lorenz RD, Lopes RM, Paganelli F, Lunine JI, Kirk RL, et al. 2008. Titan's inventory of organic surface materials. *Geophys. Res. Lett.* 35:L02206

Lorenz RD, Wall S, Radebaugh J, Boubin G, Reffet E, et al. 2006. The sand seas of Titan: Cassini RADAR observations of longitudinal dunes. *Science* 312:724–27
Lunine JI, Lorenz RD. 2009. Rivers, lakes, dunes, and rain: crustal processes in Titan's methane cycle. *Annu. Rev. Earth Planet. Sci.* 37:299–320
Lunine JI, Stevenson DJ, Yung YL. 1983. Ethane ocean on Titan. *Science* 222:1229–30
Luz D, Hourdin F, Rannou P, Lebonnois S. 2003. Latitudinal transport by barotropic waves in Titan's stratosphere. II. Results from a coupled dynamics-microphysics-photochemistry GCM. *Icarus* 166:343–58
Mastrogiuseppe M, Valerio P, Hayes A, Lorenz R, Lunine J, et al. 2014. The bathymetry of a Titan sea. *Geophys. Res. Lett.* 41:1432–37
Matsuno T. 1966. Quasi-geostrophic motions in the equatorial area. *J. Meteorol. Soc. Jpn.* 44:25–43
McKay CP, Pollack JB, Courtin R. 1989. The thermal structure of Titan's atmosphere. *Icarus* 80:23–53
McKay CP, Pollack JB, Courtin R. 1991. The greenhouse and antigreenhouse effects on Titan. *Science* 253:1118–21
Mitchell JL. 2008. The drying of Titan's dunes: Titan's methane hydrology and its impact on atmospheric circulation. *J. Geophys. Res.* 113:E08015
Mitchell JL. 2012. Titan's transport-driven methane cycle. *Astrophys. J.* 756:L26
Mitchell JL, Ádámkovics M, Caballero R, Turtle EP. 2011. Locally enhanced precipitation organized by planetary-scale waves on Titan. *Nat. Geosci.* 4:589–92
Mitchell JL, Pierrehumbert RT, Frierson DMW, Caballero R. 2006. The dynamics behind Titan's methane clouds. *PNAS* 103:18421–26
Mitchell JL, Pierrehumbert RT, Frierson DMW, Caballero R. 2009. The impact of methane thermodynamics on seasonal convection and circulation in a model Titan atmosphere. *Icarus* 203:250–64
Mitchell JL, Vallis GK. 2010. The transition to superrotation in terrestrial atmospheres. *J. Geophys. Res.* 115:E12008
Moore JM, Howard AD, Morgan AM. 2014. The landscape of Titan as witness to its climate evolution. *J. Geophys. Res. Planets* 119:2060–77
Mousis O, Schmitt B. 2008. Sequestration of ethane in the cryovolcanic subsurface of Titan. *Astrophys. J.* 667:L67–70
Muhleman DO, Grossman AW, Butler BJ, Slade MA. 1990. Radar reflectivity of Titan. *Science* 25:975–80
Müller-Wodarg I, Griffith CA, Lellouch E, Cravens TE, eds. 2014. *Titan: Interior, Surface, Atmosphere, and Space Environment*. Cambridge, UK: Cambridge Univ. Press
Neish CD, Lorenz RD. 2014. Elevation distribution of Titan's craters suggests extensive wetlands. *Icarus* 228:27–34
Newman CE, Lee C, Lian Y, Richardson MI, Toigo AD. 2011. Stratospheric superrotation in the TitanWRF model. *Icarus* 213:636–54
Niemann HB, Atreya SK, Bauer SJ, Carignan GR, Demick JE, et al. 2005. The abundances of constituents of Titan's atmosphere from the GCMS instrument on the Huygens probe. *Nature* 438:779–84
Penteado PF, Griffith CA. 2010. Ground-based measurements of the methane distribution of Titan. *Icarus* 206:345–51
Pierrehumbert R. 1995. Thermostats, radiator fins, and the local runaway greenhouse. *J. Atmos. Sci.* 52:1784–806
Pierrehumbert RT. 2010. *Principles of Planetary Climate*. Cambridge, UK: Cambridge Univ. Press
Porco C, Baker E, Barbara J, Beurle K, Brahic A, et al. 2005. Imaging of Titan from the Cassini spacecraft. *Nature* 434:159–68
Radebaugh J, Lorenz RD, Lunine JI, Wall SD, Boubin G, et al. 2008. Dunes on Titan observed by Cassini Radar. *Icarus* 194:690–703
Rannou P, Montmessin F, Hourdin F, Lebonnois S. 2006. The latitudinal distribution of clouds on Titan. *Science* 311:201–5
Rodriguez S, Le Mouélic S, Rannou P, Sotin C, Brown RH, et al. 2011. Titan's cloud seasonal activity from winter to spring with Cassini/VIMS. *Icarus* 216:89–110
Rodriguez S, Le Mouélic S, Rannou P, Tobie G, Baines KH, et al. 2009. Global circulation as the main source of cloud activity on Titan. *Nature* 459:678–82

Roe HG. 2012. Titan's methane weather. *Annu. Rev. Earth Planet. Sci.* 40:355–82
Roe HG, Bouchez AH, Trujillo CA, Schaller EL, Brown ME. 2005. Discovery of temperate latitude clouds on Titan. *Astrophys. J.* 618:L49–52
Roe HG, de Pater I, Macintosh BA, McKay CP. 2002. Titan's clouds from Gemini and Keck adaptive optics imaging. *Astrophys. J.* 581:1399–406
Rossow WB, Williams GP. 1979. Large-scale motion in the Venus stratosphere. *J. Atmos. Sci.* 36:377–89
Samuelson RE, Nath NR, Borysow A. 1997. Gaseous abundances and methane supersaturation in Titan's troposphere. *Planet. Space Sci.* 45:959–80
Schaller EL, Brown ME, Roe HG, Bouchez AH. 2006a. A large cloud outburst at Titan's south pole. *Icarus* 182:224–29
Schaller EL, Brown ME, Roe HG, Bouchez AH, Trujillo CA. 2006b. Dissipation of Titan's south polar clouds. *Icarus* 184:517–23
Schaller EL, Roe HG, Schneider T, Brown ME. 2009. Storms in the tropics of Titan. *Nature* 460:873–75
Schinder PJ, Flasar FM, Marouf EA, French RG, McGhee CA, et al. 2011. The structure of Titan's atmosphere from Cassini radio occultations. *Icarus* 215:460–74
Schinder PJ, Flasar FM, Marouf EA, French RG, McGhee CA, et al. 2012. The structure of Titan's atmosphere from Cassini radio occultations: occultations from the Prime and Equinox missions. *Icarus* 221:1020–31
Schneider T. 2006. The general circulation of the atmosphere. *Annu. Rev. Earth Planet. Sci.* 34:655–88
Schneider T, Graves SDB, Schaller EL, Brown ME. 2012. Polar methane accumulation and rainstorms on Titan from simulations of the methane cycle. *Nature* 481:58–61
Smith BA, Soderblom L, Beebe R, Boyce J, Briggs G, et al. 1981. Encounter with Saturn: Voyager 1 imaging science results. *Science* 212:163–91
Sobel AH, Bretherton CS. 2000. Modeling tropical precipitation in a single column. *J. Clim.* 13:4378–92
Stofan ER, Elachi C, Lunine JI, Lorenz RD, Stiles B, et al. 2007. The lakes of Titan. *Nature* 445:61–64
Tobie G, Lunine JI, Sotin C. 2006. Episodic outgassing as the origin of atmospheric methane on Titan. *Nature* 440:61–64
Tokano T. 2005. Meteorological assessment of the surface temperatures on Titan: constraints on the surface type. *Icarus* 173:222–42
Tokano T, McKay CP, Neubauer FM, Atreya SK, Ferri F, et al. 2006. Methane drizzle on Titan. *Nature* 442:432–35
Tokano T, Neubauer FM, Laube M, McKay CP. 1999. Seasonal variation of Titan's atmospheric structure simulated by a general circulation model. *Planet. Space Sci.* 47:493–520
Tomasko MG, Archinal B, Becker T, Bézard B, Bushroe M, et al. 2005. Rain, winds and haze during the Huygens probe's descent to Titan's surface. *Nature* 438:765–78
Tomasko MG, Bézard B, Doose L, Engel S, Karkoschka E. 2008a. Measurements of methane absorption by the descent imager/spectral radiometer (DISR) during its descent through Titan's atmosphere. *Planet. Space Sci.* 56:624–47
Tomasko MG, Bézard B, Doose L, Engel S, Karkoschka E, Vinatier S. 2008b. Heat balance in Titan's atmosphere. *Planet. Space Sci.* 56:648–59
Tomasko MG, Doose L, Engel S, Dafoe L, West R, et al. 2008c. A model of Titan's aerosols based on measurements made inside the atmosphere. *Planet. Space Sci.* 56:669–707
Trenberth K, Stepaniak D. 2003. Covariability of components of poleward atmospheric energy transports on seasonal and interannual timescales. *J. Clim.* 16:3691–705
Turtle EP, Del Genio AD, Barbara JM, Perry JE, Schaller EL, et al. 2011a. Seasonal changes in Titan's meteorology. *Geophys. Res. Lett.* 38:L03203
Turtle EP, Perry JE, Hayes AG, Lorenz RD, Barnes JW, et al. 2011b. Rapid and extensive surface changes near Titan's equator: evidence of April showers. *Science* 331:1414–17
Turtle EP, Perry JE, Hayes AG, McEwen AS. 2011c. Shoreline retreat at Titan's Ontario Lacus and Arrakis Planitia from Cassini Imaging Science Subsystem observations. *Icarus* 212:957–59
Turtle EP, Perry JE, McEwen AS, Del Genio AD, Barbara J, et al. 2009. Cassini imaging of Titan's high-latitude lakes, clouds, and south-polar surface changes. *Geophys. Res. Lett.* 36:L02204
Vallis GK. 2006. *Atmospheric and Oceanic Fluid Dynamics*. Cambridge, UK: Cambridge Univ. Press

Wheeler M, Kiladis GN. 1999. Convectively coupled equatorial waves: analysis of clouds and temperature in the wavenumber-frequency domain. *J. Atmos. Sci.* 56:374–99

Williams IN, Pierrehumbert RT, Huber M. 2009. Global warming, convective threshold and false thermostats. *Geophys. Res. Lett.* 36:L21805

Williams KE, McKay CP, Persson F. 2012. The surface energy balance at the Huygens landing site and the moist surface conditions on Titan. *Planet. Space Sci.* 60:376–85

Yung Y, Allen M, Pinto JP. 1984. Photochemistry of the atmosphere of Titan: comparison between model and observations. *Astrophys. J. Suppl.* 55:465–506

Annual Review
of Earth and
Planetary Sciences
Volume 44, 2016

Contents

Indexes

Errata

An online log of corrections to *Annual Review of Earth and Planetary Sciences* articles may be found at http://www.annualreviews.org/errata/earth